MIXED LAYER HEIGHT ESTIMATES – A STATISTICAL ANALYSIS OF ALGORITHM PERFORMANCE

THESIS

Lisa C. Shoemaker, Captain, USAF

AFIT/GM/ENP/00M-12

DEPARTMENT OF THE AIR FORCE
AIR UNIVERSITY

AIR FORCE INSTITUTE OF TECHNOLOGY

Wright-Patterson Air Force Base, Ohio

APPROVED FOR PUBLIC RELEASE; DISTRIBUTION UNLIMITED.

REPORT DOCUMENTATION PAGE

Form Approved
OMB No. 0704-0188

1. AGENCY USE ONLY *(Leave blank)*	2. REPORT DATE	3. REPORT TYPE AND DATES COVERED
	March 2000	Master's Thesis

4. TITLE AND SUBTITLE
Mixed Layer Height Estimates - A Statistical Analysis of Algorithm Performance

5. FUNDING NUMBERS
EN

6. AUTHOR(S)
Lisa C. Shoemaker, Captain, USAF

7. PERFORMING ORGANIZATION NAME(S) AND ADDRESS(ES)
Air Force Institute of Technology
Graduate School of Engineering and Management (AFIT/EN)
2950 P Street, Building 640
WPAFB OH 45433-7765

8. PERFORMING ORGANIZATION REPORT NUMBER
AFIT/GM/ENP/00M-12

9. SPONSORING/MONITORING AGENCY NAME(S) AND ADDRESS(ES)
AFTAC/TMKE
Attn: Mr. Devin Dean and Captain Robert Russ
1030 S. Hwy A1A
PAFB FL 32925-3002 DSN: 854-8921

10. SPONSORING/MONITORING AGENCY REPORT NUMBER

11. SUPPLEMENTARY NOTES
Lt Col Michael K. Walters, ENP, DSN: 785-3636, ext. 4681

12a. DISTRIBUTION AVAILABILITY STATEMENT
APPROVED FOR PUBLIC RELEASE; DISTRIBUTION UNLIMITED

12b. DISTRIBUTION CODE

13. ABSTRACT *(Maximum 200 words)*
The Air Force Technical Applications Center (AFTAC) conducts dispersion transport modeling as part of their mission support for the United States Atomic Energy Detection System. Part of that modeling effort requires knowledge of the height of the mixed layer in the lower atmosphere to determine the vertical extent through which particulates can be distributed. The mixed layer can be estimated by analyzing atmospheric profiles of parameters obtained from observations (e.g., upper air soundings) or atmospheric models. Six mixed layer algorithms were evaluated: Gradient Richardson Number (RICH), Potential Temperature (POTEMP), Potential Instability Mixing Depth (PIMIX), and three variations of the PIMIX algorithm that have never been statistically tested. The purpose of the research was to evaluate algorithm performance when observed and model-generated soundings were used to determine the height of the mixed layer. The research was divided into two sections: observed and forecast. In the observed section, observed soundings were hand-analyzed to obtain subjective mixed layer heights, which were compared to the algorithm heights. In the forecast section, soundings generated by the Regional Atmospheric Modeling System (RAMS) were subjectively analyzed, and the results were compared to the algorithms' output. Additionally, the algorithms were evaluated to determine if their performance varied temporally (i.e., was algorithm performance dependent on observation time). Finally, the algorithms' root mean square errors (RMSE) compared to the subjective heights were calculated.

14. SUBJECT TERMS	15. NUMBER OF PAGES	16. PRICE CODE
Planetary Boundary Layer, Mixed Layer, Mixed Layer Heights	122	

17. SECURITY CLASSIFICATION OF REPORT	18. SECURITY CLASSIFICATION OF THIS PAGE	19. SECURITY CLASSIFICATION OF ABSTRACT	20. LIMITATION OF ABSTRACT
UNCLASSIFIED	UNCLASSIFIED	UNCLASSIFIED	UL

AFIT/GM/ENP/00M-12

MIXED LAYER HEIGHT ESTIMATES – A STATISTICAL ANALYSIS OF ALGORITHM PERFORMANCE

THESIS

Presented to the Faculty

Department of Engineering Physics

Graduate School of Engineering and Management

Air Force Institute of Technology

Air University

Air Education and Training Command

In Partial Fulfillment of the Requirements for the

Degree of Master of Science in Meteorology

Lisa C. Shoemaker, B.S.

Captain, USAF

March 2000

AFIT/GM/ENP/00M-12

MIXED LAYER HEIGHT ESTIMATES – A STATISTICAL ANALYSIS OF ALGORITHM PERFORMANCE

Lisa C. Shoemaker, B.S.

Captain, USAF

Approved:

29 Feb 2000	
Michael K. Walters (Chairman)	Date
1 Mar 2000	
Cecilia A. Miner (Member)	Date
1 Mar 2000	
David E. Weeks (Member)	Date

Preface

I want to thank Robert Russ and Devin Dean of AFTAC for getting data to me quickly and assisting me with the funding approval for my visit to Patrick AFB to discuss this research project. Their efforts and timely responses in providing me the support and information I needed were greatly appreciated. Many thanks go to Devin for always answering my seemingly infinite number of questions pertaining to the SLAM algorithms. I also want to acknowledge my instructors (past and present) for providing classroom instruction and guidance that prepared me to venture into this project.

Very special thanks go to my family and close friends whose support and words of encouragement provided me added motivation at times when I thought I could work no further. Most importantly, I want to thank my parents for instilling in me the values of dedication and hard work. They taught me that great achievements are earned not from gratuitous handouts but rather from self-discipline, mental toughness, and sometimes personal sacrifices. This philosophy has meant the difference between success and failure for me. Thanks Mom and Dad!

Once a job is begun

Stick with it until it's done.

Be it great or be it small

Do it right or not at all.

In memory of Scott Andrew Shoemaker

Lisa C. Shoemaker

Table of Contents

List of Figures

List of Tables

Table		Page

AFIT/GM/ENP/00M-12

Abstract

The Air Force Technical Applications Center (AFTAC) conducts dispersion transport modeling as part of their mission support for the United States Atomic Energy Detection System. Part of that modeling effort requires knowledge of the height of the mixed layer in the lower atmosphere to determine the vertical extent through which particulates can be distributed. The mixed layer can be estimated by analyzing atmospheric profiles of parameters obtained from observations (e.g., upper air soundings) or atmospheric models.

Six mixed layer algorithms were evaluated: Gradient Richardson Number (RICH), Potential Temperature (POTEMP), Potential Instability Mixing Depth (PIMIX), and three variations of the PIMIX algorithm that have never been statistically tested. The purpose of the research was to evaluate algorithm performance when observed and model-generated soundings were used to determine the height of the mixed layer. The research was divided into two sections: observed and forecast. In the observed section, observed soundings were hand-analyzed to obtain subjective mixed layer heights, which were compared to the algorithm heights. In the forecast section, soundings generated by the Regional Atmospheric Modeling System (RAMS) were subjectively analyzed, and the results were compared to the algorithms' output. Additionally, the algorithms were evaluated to determine if their performance varied temporally (i.e., was algorithm performance dependent on observation time). Finally, the algorithm root mean square errors (RMSE) compared to the subjective heights were calculated.

MIXED LAYER HEIGHT ESTIMATES – A STATISTICAL ANALYSIS OF ALGORITHM PERFORMANCE

I. Introduction

1.1 Background

This thesis is a continuation of research conducted by First Lieutenant Robert Russ at the Air Force Institute of Technology, Wright-Patterson AFB, OH (19: 1999), and it is sponsored by the Air Force Technical Applications Center (AFTAC) located at Patrick AFB, FL. AFTAC is the sole DoD agency operating the United States Atomic Energy Detection System (USAEDS). Using the USAEDS, AFTAC has the mission to monitor various nuclear test ban treaties. To support that mission, AFTAC has a robust meteorological capability that includes the use of transport and dispersion models as well as mesoscale models in order to predict the location of any potential nuclear particulates associated with nuclear tests. The height of the Planetary Boundary Layer (PBL), also referred to as the height of the mixed layer in this research, is a key input in the dispersion-transport models because the PBL height largely determines the vertical extent of convective mixing (1: Alapaty et al. 1997), thereby influencing the spread of particulates within the atmosphere. Determining the height of the PBL is no trivial task, especially since definitions of the PBL vary among scientists. In general terms, the PBL is considered to be the turbulent region adjacent to the earth's surface or the transition region between the turbulent surface layer and the non-turbulent "free" atmosphere (24: Wyngaard 1986). In addition, there are direct and indirect methods that can be used to estimate the height of

the PBL. Direct methods typically rely on LIDAR (Light Detection and Ranging) or SODAR (Sound Detection and Ranging) measurements of relative differences between aerosols and particulates in the PBL and the clear air above (14: Hooper and Eloranta 1986). Indirect methods, however, depend on information derived from atmospheric data gathered from devices such as rawinsondes. The indirect methodology is the focus of this research.

As part of their dispersion and transport modeling effort, AFTAC employs the Short Range Layered Atmospheric Model (SLAM) (4: Capuano et al. 1997), which estimates PBL heights using sounding analysis algorithms that ingest observed or model forecasted upper air soundings. A drawback to using observed soundings is that they are normally only taken twice per day – 00 and 12 UTC. Depending on the geographic location of the observation site, the observation time may not coincide with the occurrence of the theoretical maximum and minimum PBL heights – just prior to sunset and shortly after sunrise, respectively (15: Kaimal et al. 1976). With the advancement in mesoscale modeling, forecasted soundings are making it possible to estimate boundary layer heights in data-sparse regions of the world and to optimize the times when forecast soundings are valid. Forecast soundings are comprised of areal averages of thermodynamic variables. Therefore, these soundings will not reflect any small scale features, and when plotted, the forecast soundings will be "smoother" than an observed sounding's plot. SLAM obtains mesoscale model data and forecast upper air soundings from the Regional Atmospheric Modeling System (RAMS) (19: Russ 1999). RAMS operates using a terrain-following vertical coordinate (sigma-z) instead of pressure (22: Walko et al. 1993). Each of the 30 RAMS data levels (heights) has associated parameters (e.g., temperature, pressure, wind) reported. These sigma-z data levels typically do not coincide with the standard upper air mandatory reporting levels. Therefore, RAMS has an internal program that interpolates between sigma-z levels to ensure that parameters are reported for

mandatory pressure levels. The significance of this procedure is explained further in Chapter 3 in the SLAM algorithm description section.

SLAM contains three main sounding analysis algorithms used to estimate the PBL height: Potential Temperature (POTEMP), Potential Instability Mixing Depth (PIMIX), and Gradient Richardson Number (RICH). These algorithms were designed to operate on observed soundings and not model-generated forecast soundings. Therefore, one can expect algorithm performance to vary depending upon whether observed or forecast soundings are ingested. In his research, Russ (19: 1999) verified that PIMIX is more suited for moist, deeply convective sounding profiles, while POTEMP's strength is in the analysis of drier atmospheric sounding profiles. Following Russ' research, AFTAC's modeling contractor, ENSCO Inc., modified the PIMIX algorithms to yield three new variations of PIMIX (PIMIX day/night, PIMIX-NM1, and PIMIX-NM2). An overview of these algorithms' design and logic is in Chapter 2. AFTAC was mostly interested in the comparisons of the new PIMIX variations since those algorithms have never been statistically analyzed. For completeness, RICH and POTEMP were included in the study.

1.2 Problem and Objective

With three additional sounding analysis algorithms available for use, AFTAC wanted answers to the following questions:

- Which of the algorithms' height estimates is most accurate when using observed soundings?
- Which of the algorithms' height estimates is most accurate when using RAMS forecast soundings?
- How do the algorithms' height estimates compare when temporally stratified?
- What is the root mean square error (RMSE) of the algorithms?

In order to answer the first two questions, 1,052 upper air soundings (525 observed and 527 RAMS) from five different geographic locations were selected in a manner to afford climatological variety and to mitigate spatial correlation, as explained in Chapter 3. Each of the soundings was subjectively analyzed to obtain an estimated height of the mixed layer. Each subjective height was considered to be the ground-truth height. The ground-truth values were compared to the heights produced by each of the SLAM algorithms. The subjective analysis process was similar to, but not exactly the same as, the method used by Russ (19: 1999). Russ' method somewhat mirrored the logic of PIMIX and POTEMP, which essentially resulted in a quality check of the algorithms. The method used in this research was different because the analytical logic did not mirror that of the algorithms. In addition, the main parameter used in the method differed from that used by Russ and the algorithms. Virtual potential temperature was selected as the analytical parameter versus potential temperature in Russ' method. The significance of virtual potential temperature in planetary boundary layer analyses is discussed in Chapter 2.

Once the subjective heights were determined, they were statistically compared to the algorithm heights using the Cochran test and confidence intervals. Tests were conducted using a combination of 00 and 12 UTC heights. Then the heights were separated by observation time to determine the statistical significance of a temporal stratification.

RMSE values were calculated for each algorithm after filtering out the soundings where an obvious thermal inversion did not exist. The logic in this approach was to assess the algorithms' ability to analyze the "easy" cases where RMSE values should be low. If the algorithms could not handle the simple cases, then it was assumed that the algorithm analyses of the more difficult cases would certainly yield extremely large RMSE values. It is important to note that the RMSE values were relative to the subjective heights. In order to get a true RMSE, the algorithm heights

should be compared to mixed layer height measurements yielded by an instrument (e.g., LIDAR, SODAR).

1.3 Importance of Research

This research provided the first statistical testing of AFTAC's three new PIMIX algorithm variations. The research results will also enable AFTAC to further its dispersion and transport modeling efforts by employing the most appropriate algorithm based upon algorithm strengths and weaknesses in particular geographical regimes and times of day. Furthermore, AFTAC will gain knowledge concerning how meaningful the algorithms' mixed layer height estimates are.

1.4 Thesis Organization

Chapter 2 offers a general overview of PBL theory and background as well as descriptions of the SLAM algorithms. Chapter 3 details the experimental methodology including the selection of data, subjective analysis process, and statistical analysis tests. Chapter 4 contains the experimental results and statistical analyses of the observed and RAMS forecast soundings. In Chapter 5, conclusions and recommendations for further research opportunities are detailed. Tables of the subjective and algorithm mixed layer heights are in Appendices D through H.

II. Theoretical Background

2.1 Overview

This chapter discusses general theory and principles governing the planetary boundary layer that are relevant to this research project. The SLAM algorithms are described in their basic mathematical forms, including modifications made to PIMIX since Russ (19: 1999) completed his research.

2.2 The Planetary Boundary Layer

As mentioned in Chapter 1, the planetary boundary layer (PBL) is generally defined as the turbulent region adjacent to the earth's surface or the transition region between the turbulent surface layer and the non-turbulent free atmosphere. One particularly obvious feature of the PBL is its diurnal cycle, which is especially evident over land. Furthermore, the diurnal variation of the PBL tends to be most evident during the summer months when daytime solar heating is at its maximum (7: Dayan and Rodnizki 1998). The general nature of the PBL is to be thinner in regions of high pressure and thicker in regions of low pressure. The subsidence associated with high pressure usually drives air out of the high and into lower pressure regions, where the upward motions tend to carry boundary layer air away from the ground to higher altitudes throughout the troposphere (21: Stull 1988).

Stull (21: 1988) describes the PBL's three major components: the stable boundary layer, the residual layer, and the mixed layer. Figure 1 illustrates the diurnal evolution of these three components. Following sunset, the mixed layer begins to decay and is transformed into the residual layer, named such because its initial mean-state variables (e.g., potential temperature) are the same as those of the recently decayed mixed layer. As the night progresses and the bottom of the residual layer is affected by the earth's surface, a stable nocturnal layer develops. The top of the stable layer is not well defined, as it blends in with the residual layer.

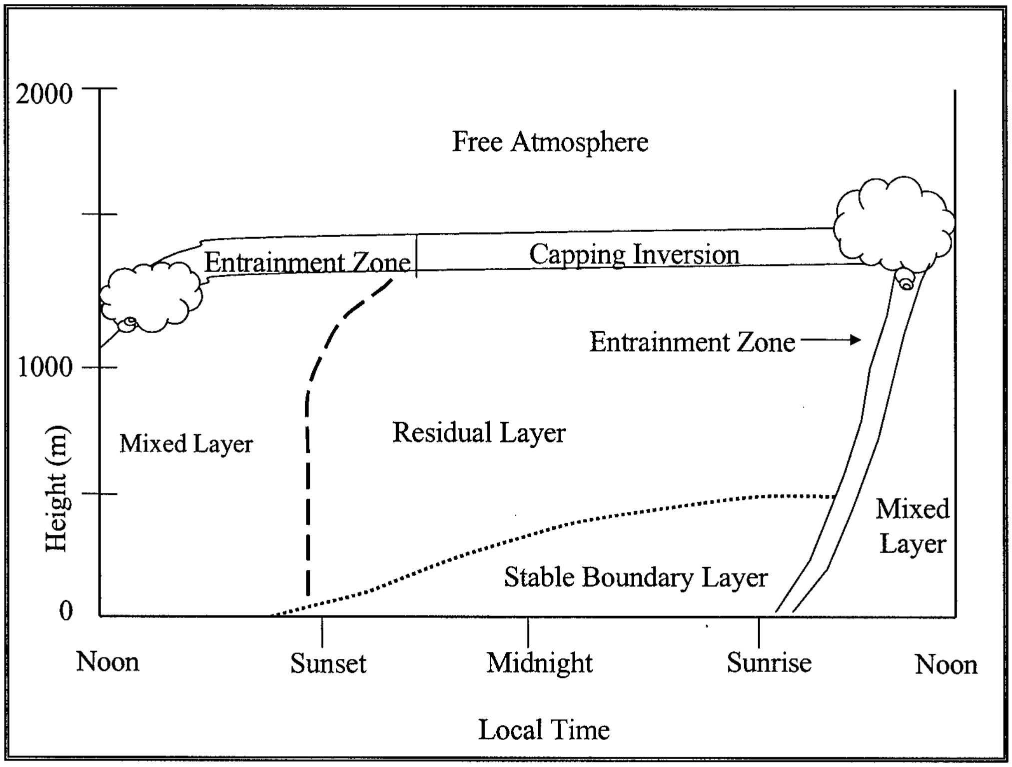

Figure 1 Idealized schematic of PBL diurnal variation over land under high pressure (adapted from Stull 1988).

Shortly after sunrise, the nocturnal inversion dissipates, and the mixed layer begins to grow, becoming statically unstable and turbulent as thermals of warm air rise from the earth's surface. Throughout the day, the mixed layer grows by entraining less turbulent air from above; and in doing so, the layer can reach a depth of 1-2 km by mid-afternoon (12: Garratt 1992) and (15: Kaimal et al. 1976). Within this well-mixed layer, turbulence tends to mix heat, moisture and momentum fairly uniformly in the vertical. As a result, potential temperature, virtual potential temperature, mixing ratio, and wind speed are conserved with respect to height (15: Kaimal et al. 1976), (2: Andre et al. 1978), (21: Stull 1988), and (12: Garratt 1992). Figure 2 provides an illustration of this concept. The mixed layer is topped by a thermal inversion that acts to suppress convective and turbulent motions.

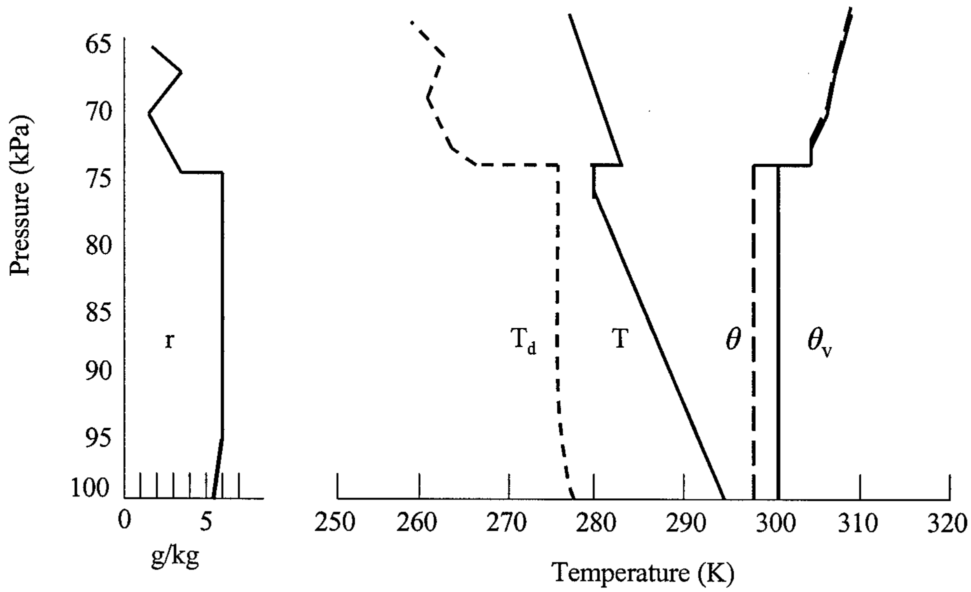

Figure 2 Example of the conservation of potential temperature (θ), virtual potential temperaure (θ_v), and mixing ratio (r) within the mixed layer. Absolute temperature (T) and dew point (T_d) are also shown (adapted from Stull 1988).

Having determined that the mixed layer is topped by a capping inversion, the next step was to determine which parameter to focus on. Several researchers, (1: Alapaty et al. 1997), (21: Stull 1988), and (12: Garratt 1992) have used virtual potential temperature profiles to study the mixed layer. Recall that virtual potential temperature is the temperature dry air must have in order to equal the density of moist air when displaced adiabatically to a pressure of 1000 mb and is defined by Equation 1, where θ is the potential temperature and r is the mixing ratio (11: Fleagle and Businger 1980).

$$\theta_v = \theta(1 + 0.61r) \tag{1}$$

As an example, water vapor is less dense than dry air. Therefore, for a given temperature, moist air is more buoyant than dry air. Since the mixed layer experiences turbulent motions affecting moisture distributions, buoyancy, and the vertical displacement of air molecules, it is reasonable to use virtual potential temperature profiles to determine the height of the PBL (21: Stull 1988). As evidenced by Equation 1, θ_v will never be less than θ. Obviously, in a very dry environment where the mixing ratio value is quite small, there is very little difference between θ and θ_v as is depicted in Figure 2. The plots of θ and θ_v are similar, but as expected, θ_v values are greater than θ in the lower, more moist portion of the sounding. Only in the very dry air above the inversion are θ and θ_v nearly equal.

The base of the θ_v inversion is frequently used to determine the depth of the mixed layer (8: Deardorff 1974), which is the basis of the subjective analysis methodology explained in Chapter 3. Figure 3 is a depiction of the θ_v profile throughout the diurnal evolution of the boundary layer.

θ_v profiles are nearly adiabatic in the middle portion of the mixed layer, while near the surface a superadiabatic layer can typically be found. The dry adiabatic lapse rate for the atmosphere is approximately 9.8°C km^{-1}; thus, a superadiabatic (SA) layer will have a lapse rate that exceeds 9.8°C km^{-1}. SA lapse rates are statically unstable with respect to vertical displacement, and they are relatively temporary events that exist in shallow layers near the earth's surface (20: Slonaker et al. 1996). SA layers typically form as a result of strong diabatic surface heating and are noticeable in the afternoon and late morning profiles when diabatic surface heating execeeds the effects of turbulent mixing.

2.3 Description of SLAM Algorithms

The SLAM algorithms were originally designed to estimate maximum mixed layer heights using observed upper air soundings. As such, the algorithms required that the input soundings have mandatory level parameters (e.g., temperature, winds,

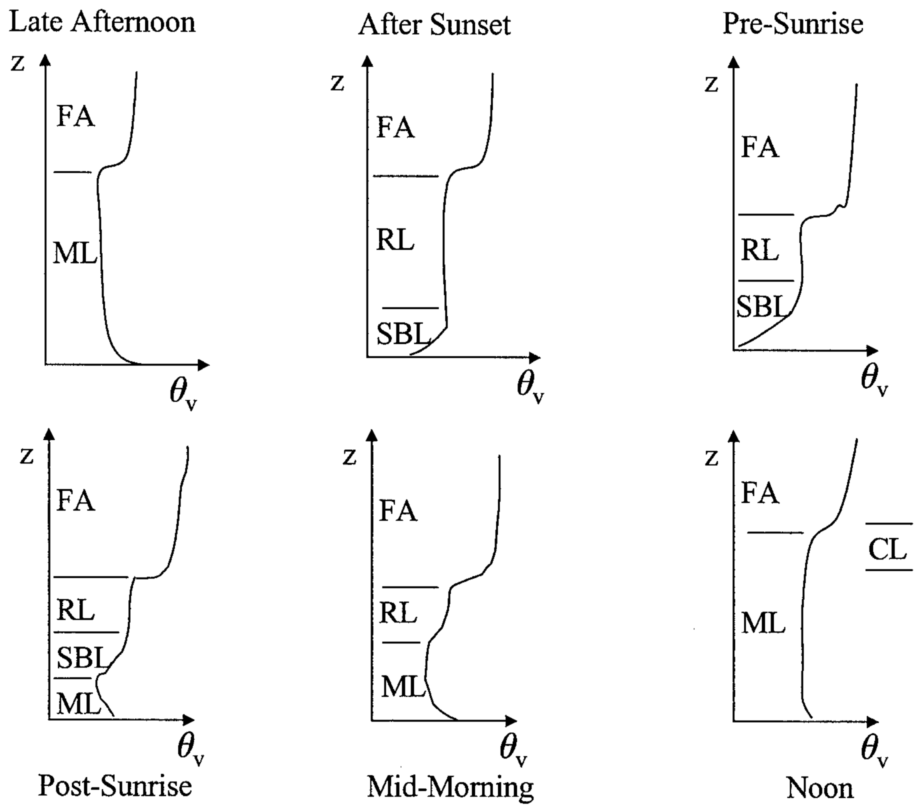

Figure 3 Idealized depiction of the diurnal evolution of θ_v boundary layer profiles. FA is free atmosphere, ML is mixed layer, RL is residual layer, SBL is stable boundary layer CL is cloud layer (adapted from Stull 1988).

and dewpoint) reported. RICH and POTEMP have remained unchanged since they were evaluated in Russ' (19: 1999) research. However, PIMIX has undergone modifications which have produced three variations of the algorithm: PIMIX day/night, PIMIX-NM1, and PIMIX-NM2. No published documentation exists for the modifications made to PIMIX; therefore, the information contained herein is provided from unofficial notes and electronic mail transmissions from ENSCO, Inc. PIMIX-NM1 and PIMIX-NM2 have been designed to estimate mixed layer heights using RAMS forecast soundings, but without relying on mandatory-level data. This is a significant departure from the other SLAM algorithms, which is why the results of this research are of interest to AFTAC.

Another important item to note is that the SLAM algorithms return mixed layer heights in meters above ground level (AGL). This distinction must be highlighted because the tools used in the subjective analysis methodology provided vertical measurements in meters above sea level (ASL). Therefore, a conversion was made from ASL to AGL, as explained in Chapter 3. When a ground-based inversion is detected, the algorithms will return a mixed layer height of $100m$, which corresponds to the SLAM height threshold.

2.3.1 Gradient Richardson (RICH) Algorithm. The Richardson number is an indicator of static stability. In general terms, it is a ratio of buoyancy forces and vertical wind shear (13: Holton 1992). The RICH algorithm is based on the gradient Richardson number, which can be calculated using the following equation (4: Capuano et al. 1997):

$$Ri = \frac{g}{\theta} \frac{\partial\theta/\partial z}{(\partial\overline{u}/\partial z)^2} \tag{2}$$

where:

- g = acceleration due to gravity ($9.8\,\mathrm{m}\,s^{-2}$),
- θ = the layer mean potential temperature (K),
- $\partial\theta/\partial z$ = the mean vertical potential temperature ($\mathrm{K}\,m^{-1}$),
- $\overline{u}$ = the layer mean wind speed ($\mathrm{m}\,s^{-1}$), and
- $(\partial\overline{u}/\partial z)$ = vertical gradient of mean windspeed (s^{-1}) .

From Equation 2, we can determine that Ri will be positive in a stable atmosphere where $\partial\theta/\partial z > 0$. Likewise, in an unstable environment where $\partial\theta/\partial z < 0$, Ri will be negative. If potential temperature is conserved vertically ($\partial\theta/\partial z = 0$), then Ri is zero. RICH calculates a values of Ri in $100m$ increments from the ground up to $4000m$ above ground level (AGL). Because RICH will not return a height value

greater than $4000m$, it is expected to be of little value when analyzing a deeply convective sounding where mixed layer heights can reach far beyond $4000m$.

The height of the mixed layer is determined by analyzing the Ri values beginning with the first value above the ground and progressing upward through the sounding levels. RICH defines the mixed layer height as the height of the first stable layer above ground where $Ri > 10$ or where $Ri > 1$ when the vertical temperature gradient is greater than $0.01\,\mathrm{K}\,m^{-1}$. RICH will return a value of $-500m$ if it cannot determine the height of the mixed layer.

2.3.2 Potential Temperature (POTEMP) Algorithm. The POTEMP algorithm computes a mixed layer height by using a series of five different potential temperature gradients ($\partial\theta/\partial z$) and five corresponding potential temperature differences ($\Delta\theta$) as defined in Table 1. POTEMP conducts a vertical search of the

$\partial\theta/\partial z_j$ (K/100m)	$\Delta\theta_j$ (K)	Mixing Depth (m)
0.3	0.9	950
0.4	1.2	1010
0.5	1.5	1049
0.6	1.8	1177
0.7	2.1	3367

Table 1 Potential temperature gradients and differences used by POTEMP. Simulated PBL heights are included (adapted from Kienzle and Masters 1990).

sounding searching for the first level at which a given $\partial\theta/\partial z$ exists. Once a layer with a given $\partial\theta/\partial z$ is located, the height within the layer of the corresponding $\Delta\theta$ is calculated using the following formula (16: Kienzle and Masters 1990) and (5: Capuano and Atchison 1985):

$$h_j = z_b + \frac{(z_t - z_b)}{(\theta_t - \theta_b)}\Delta\theta_j \tag{3}$$

where:

- $j = 1 \ldots 5$

- h_j = the intermediate mixing depth for gradient level j,
- z_t = the height of the top of the layer,
- z_b = the height of the bottom of the layer,
- θ_t = the potential temperature at the top of the layer,
- θ_b = the potential temperature at the bottom of the layer, and
- $\Delta\theta_j$ = the potential temperature difference at gradient level j.

This process is repeated for each $\partial\theta/\partial z$ value, which results in five initial mixed layer height estimates. Table 1 provides an example of this process where a height estimate is associated with each gradient value. To determine the mixed layer height, POTEMP tries to identify a discontinuity in the five height estimates. A discontinuity is defined as a difference of $200m$ or more in inversion height estimates. The mixed layer height is then defined by interpolating $\Delta\theta$ into the inversion from the base of the discontinuity. The interpolation is an attempt to account for entrainment at the top of the mixed layer. As an example using the information in Table 1, POTEMP would determine the height to be $\Delta\theta = 1.8K$ into the inversion from the $1,177m$ AGL discontinuity base. If POTEMP cannot identify a discontinuity, then the default mixed layer depth is the height associated with $\partial\theta/\partial z = 0.5K/100m$ and $\Delta\theta = 1.5K$ (16: Kienzle and Masters 1990). The application of the default procedure is depicted in Figure 4. Previous studies, (5: Capuano and Atchison 1985) and (19: Russ 1999), of POTEMP indicate that this algorithm is better suited for drier atmospheric soundings and typically underestimates the height of the mixing layer in warm, moist tropical conditions where the sounding lapse rate is less than or equal to the moist adiabatic lapse rate (16: Kienzle and Masters 1990). Therefore, in order to produce a more realistic mixed layer height estimate under tropical conditions, the PIMIX algorithm was developed.

2.3.3 Potential Instability Mixing Depth (PIMIX) Algorithm. PIMIX was designed using the same basic methodology as POTEMP, i.e., defining the mixed

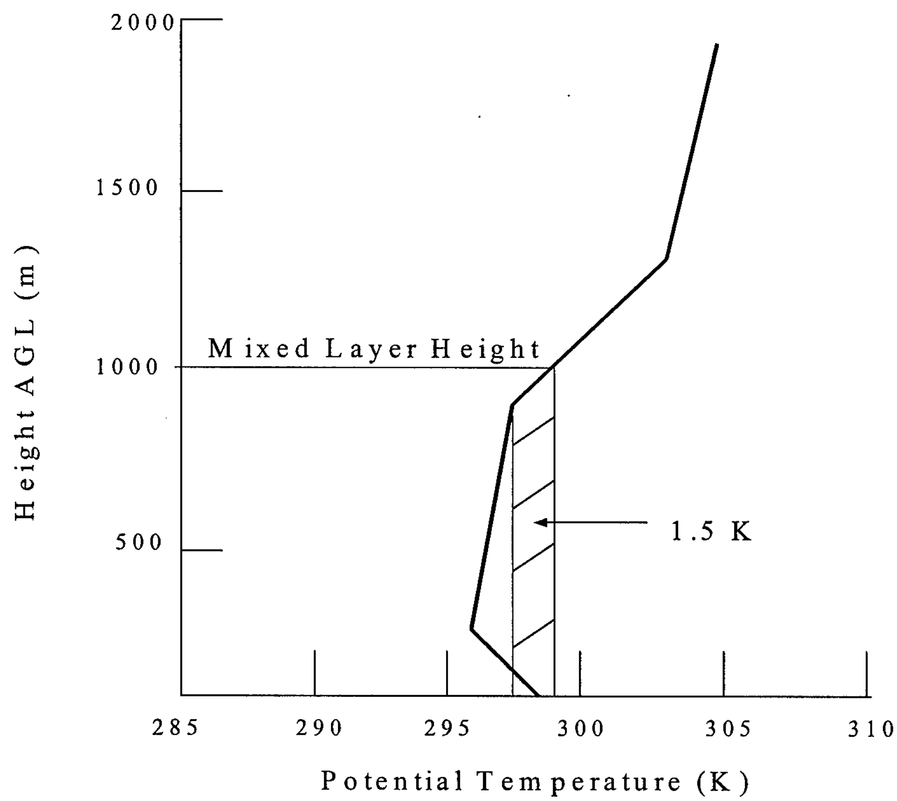

Figure 4 A graphical representation of mixed layer height estimate using POTEMP when $\partial\theta/\partial z = 0.5K/100m$ and $\Delta\theta = 1.5K$. The mixed layer height is interpolated $1.5K$ into the inversion (adapted from Kienzle and Masters 1990).

layer height as the level at which a capping inversion exists (16: Kienzle and Masters 1990). The difference between the two algorithms lies in the procedure for identifying the inversion. PIMIX compares the temperature sounding with the moist adiabatic lapse rate to find an inversion or cap on vertical mixing. The algorithm begins with the sounding's surface report and proceeds to the next reported level above the surface. PIMIX can detect a ground-based inversion, which is defined as a surface-based stable layer if the surface potential temperature is at least $5K$ less than the temperature at the top of the layer or if the stable layer is greater than $500m$ thick. A ground-based inversion is assigned a value of $100m$ by default. However, if the inversion is less than $500m$ thick or if the temperature difference between the top

and bottom of the inversion is less than $5K$, then PIMIX will ignore the inversion and attempt to locate a different one.

If no ground-based inversion is detected, the algorithm progresses up through the sounding layers until it identifies a layer whose potential temperature lapse rate is at least $0.001\,\mathrm{K}\,m^{-1}$ less than the moist adiabatic lapse rate computed for that layer. Unlike the dry adiabatic lapse rate, which is considered to be constant throughout the atmosphere, the moist adiabatic lapse rate varies. In order to calculate the layer's lapse rate, PIMIX must first calculate the saturation vapor pressure (e_s) and saturation mixing ratio (w_s) using Equations 4 and 5, where T is temperature (K) and P is pressure (mb) (16: Kienzle and Masters 1990).

$$e_s = 6.1078 \exp 17.26939 \frac{(T - 273.15)}{(T - 35.85)} \tag{4}$$

$$w_s = \frac{(0.62198 e_s)}{(P - e_s)} \tag{5}$$

PIMIX then computes the moist adiabatic lapse (γ_s) rate for the layer by substituting the values of e_s and w_s into equation 6

$$\gamma_s = \Gamma_d \frac{1 + (L w_s)/(R_d T)}{1 + (0.62198 L^2 w_s)/(R_d C_p T^2)} \tag{6}$$

where the constants

- Γ_d = dry adiabatic lapse rate,
- L = Latent heat of vaporization,
- C_p = specific heat of air at constant pressure, and
- R_d = gas constant for dry air.

Thus, if the layer lapse rate is at least $0.001\,\mathrm{K}\,m^{-1}$ less (warmer) than the calculated γ_s, then PIMIX checks to ensure the layer is thick enough to form a cap

on vertical mixing. If the difference between the potential temperature at the top and bottom of the layer is greater than $1.5K$, then the height of the mixed layer is determined to be within the layer at the level $1.5K$ into the inversion; see Figure 5. Just like POTEMP, the mixed layer height is not defined at the inversion base to

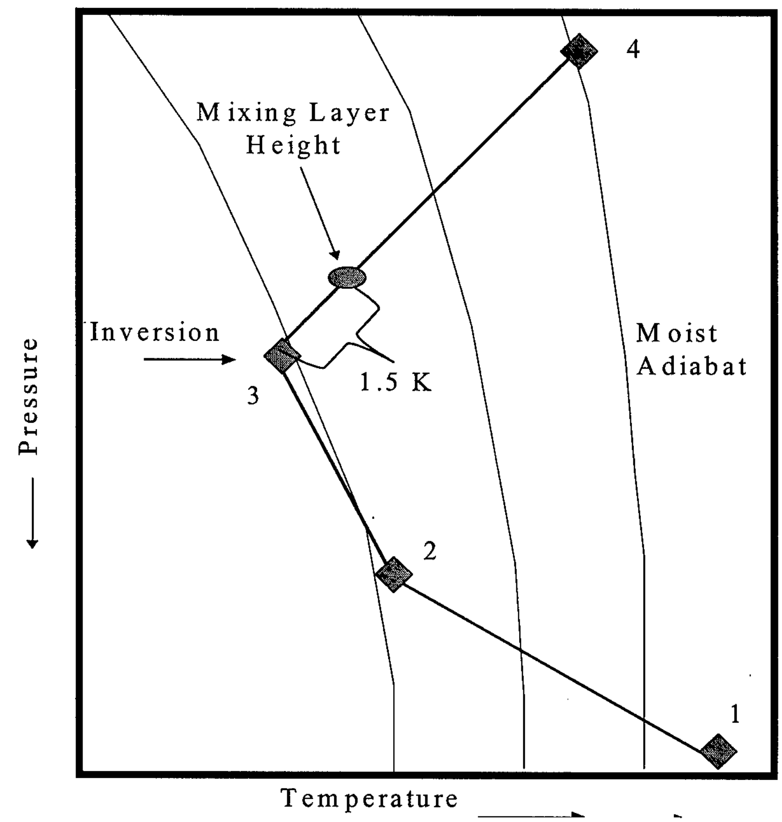

Figure 5 PIMIX schematic. The numbers represent sounding levels. For each layer, PIMIX computes a moist adiabatic lapse rate and compares it to the observed temperature lapse rate. If an inversion exists and is strong enough act as a cap on convection, then the mixed layer height is interpolated $1.5K$ into the inversion (adapted from Kienzle and Masters 1990).

allow for entrainment (16: Kienzle and Masters 1990). If the potential temperature differential in the inversion is not greater than $1.5K$, then the algorithm continues to proceed upward through the sounding to the next layer, at which point the whole process is repeated. If no layer meeting the $1.5K$ differential criteria is found, then PIMIX will return a default value of $9999m$.

2.3.4 PIMIX day/night. PIMIX day/night was the first modification made to the original PIMIX algorithm. Day is defined as 0800-2000 local standard time; likewise 2000-0800 local standard time is defined as night. The premise behind PIMIX day/night's development was to alter the algorithm's treatment of ground-based inversions at night. The algorithm will not skip over a ground-based nighttime inversion that is less than $500m$ thick; however, there must be at least a $5K$ temperature difference between the top and bottom of the inversion. During the daytime, PIMIX day/night will ignore a ground-based inversion that is less than $500m$ and search for another capping inversion. Thus, for daytime soundings PIMIX day/night uses the same logic as the original PIMIX algorithm.

2.3.5 PIMIX-NM1 and PIMIX-NM2. As previously stated, PIMIX-NM1 and PIMIX-NM2 have been created to use RAMS forecast sounding input without mandatory pressure level data reported. Both algorithms follow the same analysis logic contained in PIMIX day/night. However, PIMIX-NM2 does not interpolate the mixed layer height $1.5K$ into the inversion as do the other PIMIX variations. AFTAC and ENSCO have noted cases in past analyses in which PIMIX using RAMS data would skip over low-level inversions because the RAMS soundings had very thin lower levels (on the order of $50m$ to $200m$). Because the layers were so thin, the potential difference between the bottom and the top of the layer would be less than the required $1.5K$. Therefore, in order to account for the thin lower layers, the $1.5K$ difference was eliminated in PIMIX-NM2.

III. Experimental Design

3.1 Overview

This chapter describes the experimental design used in this research. This research is divided into two main parts: observed analysis and forecast analysis. Observed analysis involves the comparison of subjective mixed layer heights to the mixed layer heights produced by the SLAM algorithms when observed upper air soundings were used. In the forecast analysis, the SLAM algorithms used RAMS forecast upper air soundings to generate mixed layer heights, which were then compared to the mixed layer heights obtained by subjectively analyzing the RAMS upper air soundings.

3.2 Data Selection

The data used in this research are essentially the same as those used by Russ (19: 1999). Data selection was based upon the need to include a variety of climatological and meteorological regimes. A large data set was also important to ensure the results had statistical significance. For the purpose of this research, mitigating spatial and temporal correlations was a necessity. Thus, the locations used to obtain upper air information and the dates and times that the data were collected were chosen in a manner to minimize spatial and temporal correlation while covering a variety of climatological regimes.

The spatial domain for this project is defined by the following upper air reporting locations within the U.S. (WMO / ICAO / station elevation in meters); see Figure 6:

- Key West, FL (772201 / KEYW/ 6 m)
- Lake Charles, LA (72240/ KLCH/ 10 m)
- Vandenburg AFB, CA (north) (72393/ KVBG/ 112 m)

- Vandenburg AFB, CA (south) (74606/ KVBG/ 112 m)
- Grand Junction, CO (72476/ KGJT/ 1475 m)
- North Platte, NB (72562/ KLBF/ 849 m)

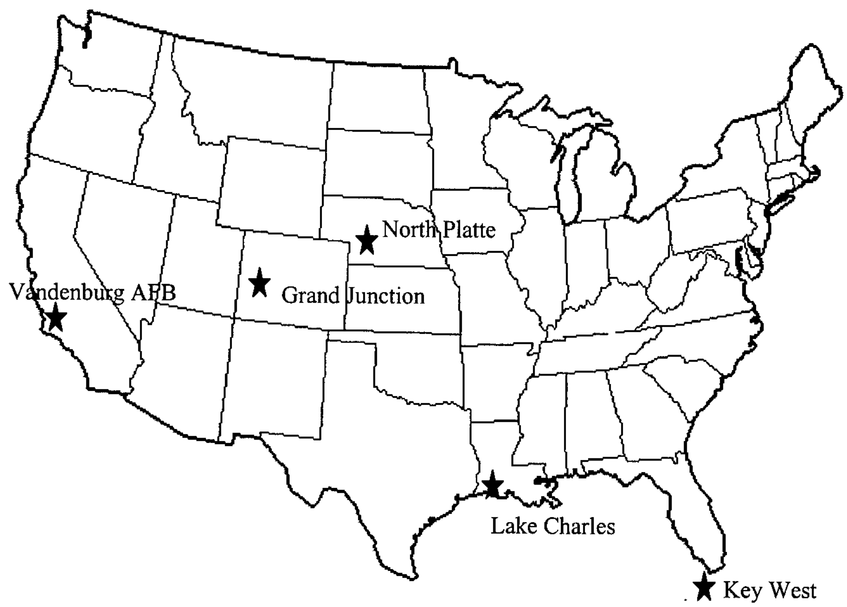

Figure 6 US map of upper air obervation reporting stations used in this research.

This spatial domain is the same as that defined by Russ (19: 1999) with the exception of the south Vandenburg site. Vandenburg AFB typically launches rawinsondes from two locations daily– the north and south observation sites. Upper air observations are generally obtained from the north site at 00 UTC, while 12 UTC observations typically come from the south site. By including the observations from the south Vandenburg location, data gaps in Russ' research were filled to provide a larger data set, which was needed to afford statistical significance. Geographically, the locations in the domain were widely separated so that spatial correlation was essentially eliminated. However, the two Vandenburg sites were counted as one single location since they are only a few hundred meters apart. The locations also offered a variety of climatological and meteorological regimes from maritime, to

mountainous, to continental (19: Russ 1999). Having solved the spatial correlation problem, focus was then shifted to the temporal aspects.

The data used in this research were obtained from calendar year 1996 and were selected in a manner to avoid temporal correlation as much as possible. Russ (19: 1999) offers an in-depth explanation of how the time correlation was mitigated. To summarize the process, data from observed and RAMS upper air soundings were collected every 10 days beginning with calendar day 10 and running through calendar day 360. A total of three soundings were collected covering a 36-hour time block every 10 calendar days. For example, the day 10 data included a 00 and 12 UTC sounding as well as a 00 UTC sounding from calendar day 11.

3.3 Subjective Analysis Technique

The 525 observed and 527 RAMS forecast upper air soundings were subjectively analyzed using the National Centers Advanced Weather Interactive Processing System (N-AWIPS), which runs on a UNIX workstation. N-AWIPS contains a graphical user interface software package called the General Meteorological Package (GEMPAK), which is a set of programs and graphic routines that can be used to decode, analyze, and display meteorological data (18: NCEP 1996). The observed soundings and the RAMS forecast upper air soundings had to be converted into GEMPAK format, which was done by AFTAC for this research. GEMPAK will not ingest sounding in the typical TTAA/TTBB upper air observational format. Once in GEMPAK format, the soundings were analyzed using the GEMPAK sounding analysis program, SNPROF. An example of the SNPROF format is in Appendix I.

Using SNPROF, a skew-T diagram of the sounding data was plotted to get an estimate of the mixed layer height (looking for a capping inversion) and to determine if there was a ground-based inversion; see Figure 7. If a ground-based inversion was identified, then the mixed layer height was estimated to be 100 m, in accordance with the SLAM algorithms' logic. If no ground-based inversion was identified, virtual

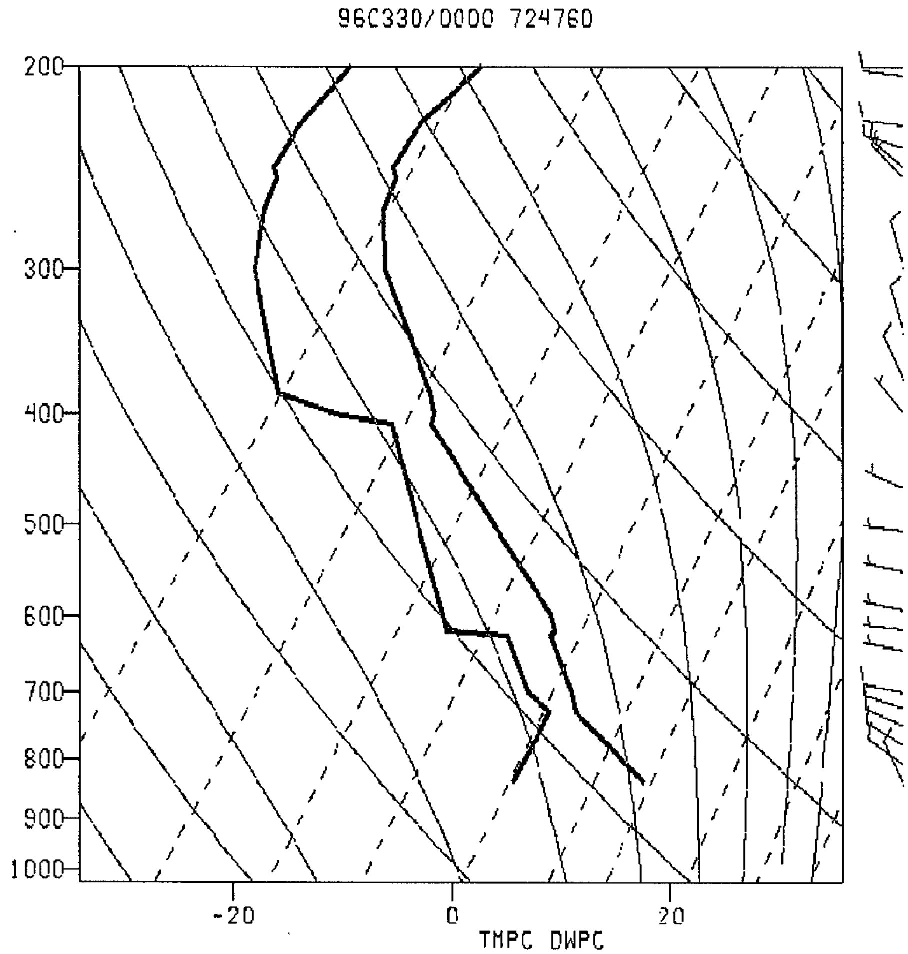

Figure 7 GEMPAK's Skew-T plot for Grand Junction, CO on 30 Mar 96 at 00 UTC. Note the capping inversion at approximately 650mb.

potential temperature (θ_v) versus height was plotted and analyzed to identify a θ_v inversion. An inversion was defined as having a lapse rate of approximately $0.01\,\mathrm{K}\,m^{-1}$ or greater. The mixed layer height was then estimated to be height of the base of the θ_v inversion. It is important to note that GEMPAK heights are given in meters above sea level (ASL). The SLAM algorithms' height estimates are given in meters AGL. Therefore, the ground truth height needed to be in meters AGL so that it could be compared to the algorithms' heights. To accomplish this, the station elevation was subtracted from the height obtained from the θ_v plot to yield an AGL height estimate (8: Deardorff 1974). Figure 8 aids in illustrating this

point. Notice the θ_v inversion at about 675 m ASL. The ground truth PBL height for this sounding was estimated to be 563 m (675 m minus the station elevation of 112 m).

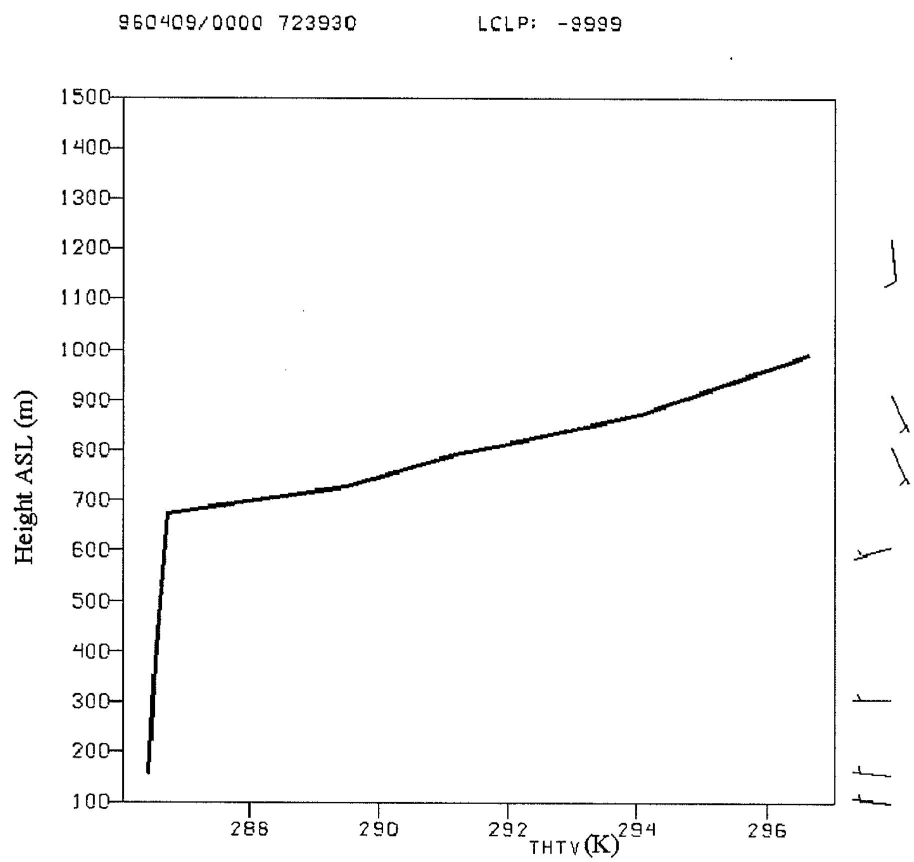

Figure 8 Example of a virtual potential temperature profile produced by SNPROF program in GEMPAK for Vandenburg AFB, CA on 9 Apr 96 at 00 UTC.

For some soundings, it was difficult to identify a θ_v inversion, especially in cases of deep convection where the lower atmosphere became thoroughly mixed up to higher altitudes and generated "noise" in the upper air observations. The terminology of noise used in this research refers to the sounding's variability; it has nothing to do with unresolved data. For the deep convection cases, when an inversion was identified it generally was above 5000m AGL. Under those circumstances, the ground truth was estimated to be 5000m, with no detailed analysis conducted

at levels above $5000m$. This resulted in no ground truth values greater than $5000m$. The logic in this methodology is a result of the scheme used to categorize data, which is explained in the next section.

3.4 Data Categorization Methodology

Having established the ground truth for each of the observed and RAMS forecast upper air soundings, a categorization method for the data was defined. First, the absolute error between the ground truth and each of the SLAM algorithms was computed. The absolute error (AE) was defined as follows, where GT is the ground truth and ALGHT is the height computed by a SLAM algorithm: $AE = |(GT - ALGHT)|$. Then, each of the absolute errors were placed into one of two categories which were defined according to AFTAC's specification. These categories differ from those used by Russ (19: 1999), where a four-category scheme to was used to evaluate algorithm performance in deeply convective and mildly convective boundary layers. The results of Russ' study indicated that the total number of categories could be reduced to two by combining the two convective categories into a single hit category. In this research, the two absolute error categories were defined as follows:

- Algorithm Hit: If the algorithm's mixed layer height estimate was within $100m$ of the ground truth, i.e., the absolute error was less than or equal to $100m$, then the algorithm's height was considered to be a hit.
  - If the ground truth $\geq 5000m$ **and** the algorithm height estimate $\geq 5000m$, then the algorithm height was considered to be a hit regardless of the magnitude of absolute error.
- Algorithm Miss: If the algorithm's mixed layer height estimate was not within $100m$ of the ground truth, i.e., the absolute error $> 100m$, then the algorithm's height was deemed a miss.

– If the algorithm failed, it was counted as a miss.

With the algorithm hits and misses calculated, it was possible to develop an analysis method that would aid in determining if there was any statistical significance in the algorithms' performances. For the purpose of accounting and to facilitate incorporation into a statistical analysis scheme, an algorithm hit was assigned a "1", while a miss was assigned a "0".

3.5 Statistical Analysis

This section provides details of the development of the hypothesis tests for both the observed and forecast portions of the research. The methodology used to determine the SLAM algorithms' RMSE relative to the ground truth estimates is also explained.

3.5.1 Hypothesis Testing. Wilks (23: 1995) suggests that the development of a hypothesis test should include a statement of the null and alternate hypotheses, as well as the selection of a test statistic with an appropriate decision rule. Because the focus of this research was to assess the relative performance of the SLAM algorithms, the hypotheses were stated as follows:

- Null Hypothesis: All of the SLAM algorithms are the same (i.e., the numbers of hits are statistically the same).
- Alternate Hypothesis: At least two of the SLAM algorithms are different (i.e., the numbers of hits are statistically different).

If the null hypothesis is rejected when in fact it is true, then a type I error is made. In order to minimize the probability of a type I error, an alpha (α) = .01 was used. This meant that there was only a one percent chance of rejecting the null hypothesis when it was true. With the hypotheses stated and an α determined, the next step involved selecting an appropriate test statistic.

Since the algorithm hits and misses were assigned as "1"s and "0"s respectively, one possible statistical approach could have been the use of a χ^2 contingency table, as was used by Russ (19: 1999). However, in order to detect more subtle differences between the algorithms, and thus increase the strength of the test, the Cochran test was used for the statistical analyses of the SLAM algorithms (6: Conover 1980).

The use of the Cochran test applies to dichotomous variables and often appears in a correlated-observations design (17: Marascuilo and McSweeny 1977). Hence, the rationale for assigning "1" and "0" to the SLAM algorithm hits and misses is justified. Table 2 is an example of how the dichotomous hit and miss table (or matrix) can be constructed. Each column in the table represents a treatment, and each row

	Alg1	Alg2	Alg3	Alg4	Alg5	Alg6
Snd1	1	0	1	0	0	1
Snd2	1	0	0	1	1	0
Snd3	0	1	0	1	1	0
Snd4	0	0	1	0	1	0

Table 2 Example of a dichotomous outcomes table

represents a block. For this project, the SLAM algorithms served as treatments, while each individual sounding was considered to be a block. The size of the tables varied based upon the number of upper air soundings that were reported at each individual obervation site. To understand how the values in Table 2 were referenced in the Cochran test, see Table 3 (6: Conover 1980). The column totals provided

Treatments	1	2	....	...	j	RowTotals
Block(1)	X_{11}	X_{12}	...	...	X_{1j}	R_1
Block(2)	X_{21}	X_{22}	...	...	X_{2j}	R_2
...	...	...	...	...	...	...
Block(r)	X_{r1}	X_{r2}	...	...	X_{rj}	R_j
ColumnTotals	C_1	C_2			C_j	$N = GrandTotal$

Table 3 Cochran's test table of key variables

the number of "hits" for each algorithm, enabling a hit rate (HR) to be calculated

for each algorithm by using equation 7.

$$HR_j = \frac{C_j}{r}. \tag{7}$$

The test statistic, T, for the Cochran test was calculated using the data from Table 2 in equation 8 (6: Conover 1980).

$$T = \frac{c(c-1)\sum_{j=1}^{c} C_j^2 - (c-1)N^2}{cN - \sum_{i=1}^{r} R_i^2} \tag{8}$$

T was then compared to a χ^2 random variable with (c-1) degrees of freedom (DF). Chi-square could be determined from statistical tables or software using $\alpha = .01$ and (c-1) DF. In the observed portion of the research, four algorithms were tested, which resulted in (4-1) DF. Using Devore's Table A.6 (9: 1995) or any statistical software, the critical χ^2 value for $\alpha = .01$ and 3 DF is 11.35. Likewise, in the forecast section of the research, six algorithms were tested giving $(6-1)$ DF and a critical χ^2 value of 15.09.

Having stated the hypotheses and identified the test statistic, a decision rule was established. The Cochran test stipulates that if the test statistic (T) is greater than the critical χ^2 value, then the null hypothesis is to be rejected in favor of the alternate. Otherwise, the null hypothesis is accepted. Thus, in this research, if T was greater than the critical χ^2 value, then the null hypothesis (all algorithms were the same) was rejected in favor of the alternate (at least two of the algorithms were different). Otherwise, the null hypothesis was accepted. The Cochran test only indicated if there were or were not differences between the algorithms. It did not provide any information about which algorithms differed. To resolve this problem, Marascuilo and McSweeny (17: 1977) suggest conducting a pairwise comparison, similar to the Tukey method (9: Devore 1995), to examine the magnitudes of relative differences between the algorithms. This process was only used when the Cochran test indicated the algorithms were different.

To perform a pairwise comparison, a method to determine confidence intervals was established based on the Cochran test post hoc procedures described in Marascuilo and McSweeny (17: 1977). The typical confidence interval usually has the following setup: $Interval = mean \pm A\sqrt[2]{Variance}$, where A is some specified statistical critical value (e.g., χ^2 or z). With this understanding, a variance was computed for each observation location by substituting data from tables similar to Table 3 in Equation 9.

$$Var = \frac{2\sum_{i=1}^{c} C_i - \sum_{i=1}^{c} C_i^2}{r^2(c-1)} \tag{9}$$

Each C_i represents a sum of algorithm hits, r is the number of observations, and c is the number of algorithms tested. Next, an appropriate statistical critical value (A) was selected. Marascuilo and McSweeny (17: 1977) state that a choice of two "statistics" can be used. One is the statistic, call it S, produced by using a variation of the Scheffé technique where $S = \sqrt[2]{\chi^2}$. The critical χ^2 value used in this technique is the same χ^2 value used in the hypothesis testing. A second statistic, the Dunn-Bonferroni (DB), can also be used (10: Dunn 1961). DB is dependent on the number of pairwise comparisons being made. For example, if four algorithms were compared, then there would be $\left[\binom{4}{2}\right] = 6$ pair comparisons made. Likewise, if six algorithms were compared, there would be 15 pairwise comparisons made. The DB statistic produces narrower confidence intervals than does the S statistic (10: Dunn 1961) and (17: 1977). Therefore, in order to ensure a greater distinction between algorithms, the DB statistic was used in the confidence interval computations. DB values were obtained from Table A-1 in Marascuilo and McSweeny (17: 1977).

Having computed the variance and critical statistical values, all that remained was to establish a method for computing a mean so that the confidence intervals could be constructed. Following Marascuilo and McSweeny (17: 1977), the simplest approach was to take each hit rate (defined as the mean of the column totals in Table 3) and form them into pairs. For the case of the four-algorithm comparison, there

were six pairs of hit rates (HR) calculated using Equation 7 that could be written as Table 4.

(HR_1, HR_2)	(HR_2, HR_3)
(HR_1, HR_3)	(HR_2, HR_4)
(HR_1, HR_4)	(HR_3, HR_4)

Table 4 Example of a pairwise comparison table.

For each HR pair, a difference of the pair values $(HR_1 - HR_2)$, $(HR_1 - HR_3)$, etc., were calculated. Those differences represented the "means" for the confidence interval computations. Thus, a confidence interval for each of the six pairs of algorithms could be computed by using the following formula where DB is the Dunn-Bonferroni value, Var is the variance computed from Equation 9, and $j \neq k$:

$$CI = (HR_j - HR_k) \pm DB\sqrt[2]{Var} \tag{10}$$

If the upper and lower bounds of CI "hooked" zero (i.e., zero was between the upper and lower bounds), then it was determined that there was no statistical difference between the two algorithms being compared. More precisely, there was no difference in the algorithms' height estimates. If CI did not include (hook) zero, then the conclusion was that there was indeed a difference between the two algorithms. As with any hypothesis test, there were a few cases in which the tests were inconclusive, leaving the tester to make a judgment call. Not all test results are simple "black and white"; occasionally "gray" areas are encountered. In this research, the gray areas occurred when the Cochran test determined that there was a difference between algorithms, yet the CI analysis failed to identify any differences between the pairs of algorithms even though the Dunn-Bonferroni values were used to generate narrower, more discriminating intervals. This type of failure only occurred three times (only in the observed section) in the research. The exact cause of the failures was not identified, but it suggested that for a given sample size, there was a minimum value

of T for which the CI methodology was powerful enough to key in on the differences in the pairs of algorithms.

3.5.2 Algorithm RMSE Computation. During the subjective analyses of the 525 observed and 527 RAMS soundings, each sounding was categorized as either easy or difficult depending on the relative ease in identifying an inversion in the virtual potential temperature profile or a ground-based inversion on the Skew-T diagram. If an inversion was readily apparent, the sounding was placed in the easy category; otherwise, it was considered to be a difficult sounding. The easy cases were used to compute the RMSE for algorithm mixed layer height estimates. Also, cases where both the subjective and algorithm heights were $\geq 5000m$, were not included in the RMSE calculations. The logic in doing so was to avoid having the errors for the easy cases masked by the expected large errors in heights for the both the difficult and the deep convection cases. For example, even a moderate absolute error of $100m$ effectively becomes an error of $10,000m^2$ in the RMSE calculation.

RMSEs were computed using the following formula where OBS was the subjective height, ALG was the algorithm height, and N was the number of "easy" soundings for the location (3: Brooks and Doswell 1996):

$$RMSE = \left[\frac{\sum_{i=1}^{N}(OBS - ALG)^2}{N}\right]^{1/2} \tag{11}$$

In addition, the "easy" soundings at each location were separated by time (00 UTC and 12 UTC), and RMSEs were computed for each time grouping to determine if the algorithms favored any particular sounding time.

Although only the "easy" cases were used in the RMSE calculations, there were still instances in which there were disparities between the truth and algorithm height estimates. Generally, if the virtual potential inversion was very distinct, then the agreement between the truth and algorithms was "good." Such was the case for the

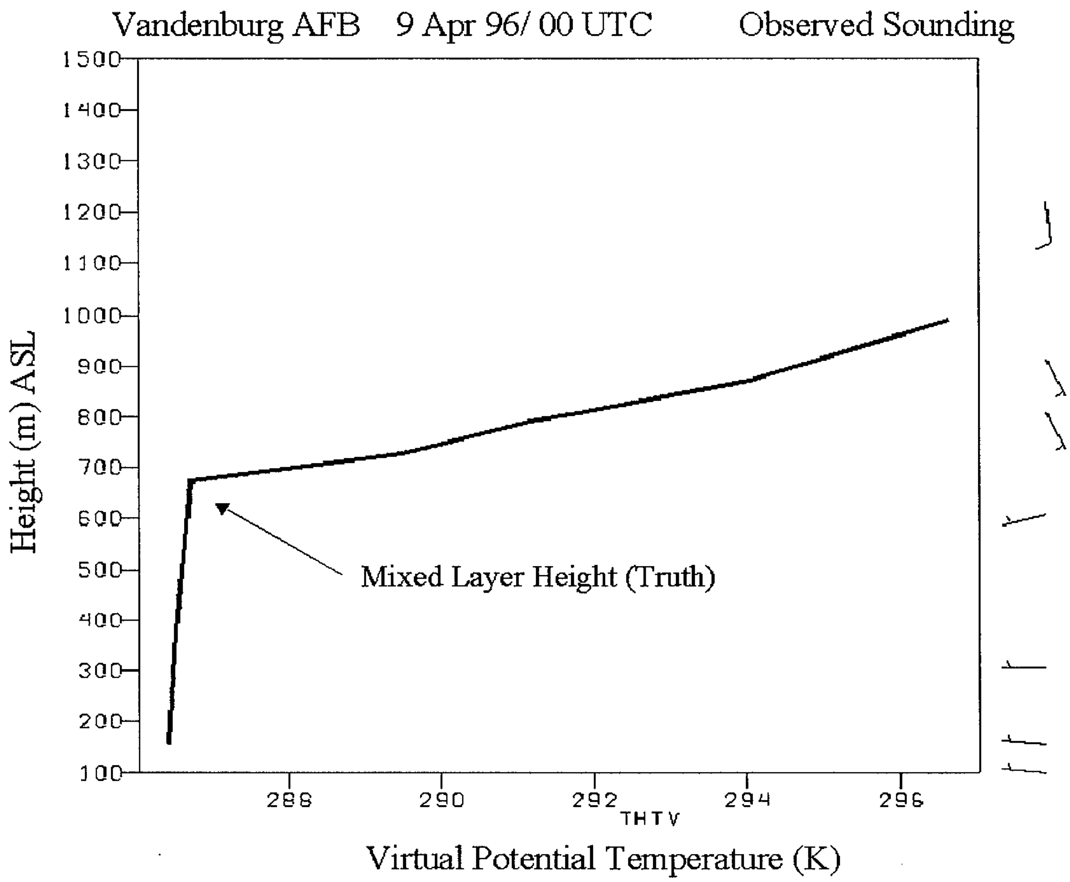

Figure 9 GEMPAK plot of θ_v with "good" agreement between truth (563m), RICH (600m), POTEMP (606m), PIMIX (605m), and PIMIX day/night (605). Reported heights are ASL height minus station elevation (112m).

virtual potential temperature plot for Vandenburg AFB, CA, in Figure 9 where the inversion was very well defined and the differences between the truth and algorithms were less than $50m$. However, if the virtual potential temperature inversion was not distinct and readily apparent to the researcher (and the algorithms), then the agreement between the truth and algorithm heights was generally poor.

An illustration of one such case can be found in Figure 10. The virtual potential temperature profile for Lake Charles, LA, does not have a distinct inversion like that of Figure 9. The resulting truth and algorithm mixed layer height estimates were consequently in poor agreement, with the largest discrepancy of over $1700m$ between truth and PIMIX day/night. Because a limited number of the soundings

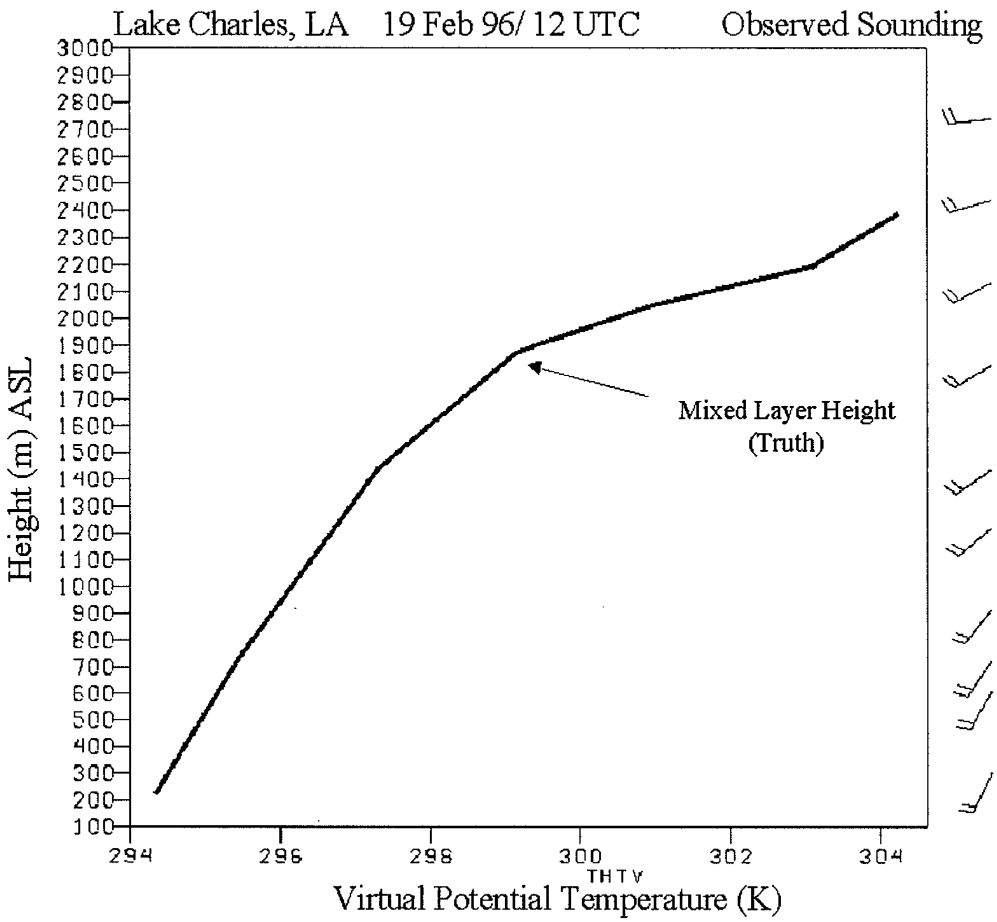

Figure 10 GEMPAK plot of θ_v with "bad" agreement between truth (1890m), RICH (800m), POTEMP (1019m), PIMIX (1984), and PIMIX day/night (100). Reported heights are ASL height minus station elevation (10m).

analyzed had well-defined inversions (even for the "easy" cases), the RMSE values were not as small as anticipated. It was expected that by using the "easy" cases RMSE values would be less than 200m. Unfortunately, those results were only realized in a few instances, which are identified in Chapter 4.

IV. Observation and Forecast Results

4.1 Overview

This chapter contains the analyses and results for the observed and forecast portions of this research. The observed and forecast sections are organized by observation location, and the analyses for each location are separated by the sounding observation times.

4.2 Observation Results

In this section, the 525 subjective mixed layer height estimates were compared to the RICH, POTEMP, PIMIX day/night, and PIMIX heights. This resulted in six pairwise comparisons, as discussed in Chapter 3. The critical χ^2 value was 11.35 for all tests conducted in this section. The number of hits, hit rate, and RMSE for each algorithm were calculated For each algorithm, three RMSEs were computed: one for the 00 UTC and 12 UTC observations combined, one for the 00 UTC, and one for the 12 UTC soundings. The numerical results of the statistical analyses of the observed soundings are provided in Appendix B.

4.2.1 Key West, FL. There were 105 soundings analyzed for Key West, FL, with 52 soundings from 00 UTC and 53 from 12 UTC. The absolute errors were categorized, as described in Chapter 3, and the Cochran test was used to determine if the SLAM algorithms' performances could be considered statistically equivalent for this location. If the algorithms were statistically different, then confidence interval (CI) evaluations were performed. Algorithm hits, hit rates, and RMSE were also computed using the methodology described in Chapter 3.

4.2.1.1 Results for 00 and 12 UTC Combined. The Cochran test was run using all observations without any time delineation. The results of the test and the pairwise comparisons of the algorithms based upon the CI evaluation are

included in Appendix B, Table 7. The algorithm hit rate, total hits, and RMSE are in Table 8. The Cochran test ($T = 58.65$) suggests that at least two of the algorithms were different, and the CI analyses indicated that the following pairs of algorithms were statistically the same: (RICH, POTEMP) and (PIMIX day/night, PIMIX). The PIMIX and PIMIX day/night RMSE values were much larger than those of POTEMP and RICH, which may be attributed to the difficulty in analyzing soundings for a tropical environment where convective processes create variability in the sounding profile. The PIMIX algorithms were expected to return larger height estimates compared to POTEMP and RICH, and thus would have a wider range of variability which could cause the RMSE values for the PIMIX algorithms to be considerably larger than for POTEMP and RICH. As anticipated, both of the PIMIX algorithms outperformed RICH and POTEMP in this tropical environment when comparing hit rates; see Table 8. Unexpectedly, PIMIX registered 49 hits, while PIMIX day/night had 45.

4.2.1.2 Results for 00 UTC. Table 9 provides the numerical results of the Cochran test and the CI analyses when only the 00 UTC observations were evaluated. The test results indicated that at least two of the algorithms were different. For this analysis, the value of T decreased, which implied that the algorithm differences weren't as pronounced as in the test using both 00 UTC and 12 UTC observations. The CI analyses showed that two pairs of algorithms were statistically different: (RICH, PIMIX day/night) and (RICH, PIMIX). PIMIX and PIMIX day/night had the same number of hits (21), followed by POTEMP (12) and RICH (7). All of the algorithms had very large RMSE values; see Table 10; however, PIMIX had the lower RMSE of the four algorithms.

4.2.1.3 Results for 12 UTC. Based upon the results of the Cochran test, there were differences between the algorithms; see Table 11. The value of T increased to 39.0 for this test, which implied that the differences between the algorithms

were more pronounced than for the 00 UTC case. Based upon the CI analyses, three pairs of algorithms were statistically different: (RICH, PIMIX day/night), (RICH, PIMIX), and (POTEMP, PIMIX). Once again, PIMIX registered more hits than any of the other three algorithms. PIMIX day/night was expected to register more hits than PIMIX because shallow ground-based inversions would not be skipped in the algorithm's analysis of the "nighttime" soundings. RMSE values for 12 UTC were significantly lower compared to the 00 UTC RMSE; see Table 12. 00 UTC at Key West correlates to 1900 local standard time, while 12 UTC correlates to 0700 local. The reduced RMSE values might be explained by the decreased probability of convective activity, and thus less noise in the soundings, at Key West during the 12 UTC hour than the 00 UTC hour. In theory, less noise in the sounding would make it easier to assess the height of the mixed layer.

4.2.2 Lake Charles, LA. There were 105 soundings analyzed for Lake Charles, LA, with 52 soundings from 00 UTC and 53 from 12 UTC. Once again, PIMIX accrued more hits than either of the other three algorithms evaluated. Algorithm RMSE values were similar to those for Key West, FL. In addition, the algorithm hit rates were comparable to those for Key West, and for both locations PIMIX registered more hits than PIMIX day/night.

4.2.2.1 Results for 00 UTC and 12 UTC Combined. The Cochran test result ($T = 41.80$) suggests that there were differences in the algorithms, and the CI analyses indicate that all of the algorithm pairs were the same with the exception of the following: (RICH, POTEMP), (POTEMP, PIMIX), and (PIMIX day/night, PIMIX); see Table 7. As expected, both of the PIMIX algorithms registered more hits than RICH and POTEMP in this maritime environment. PIMIX had the lowest RMSE value of all algorithms followed by POTEMP, PIMIX day/night, and RICH.

4.2.2.2 Results for 00 UTC. While the Cochran test indicated that there was a difference in the algorithms for the 00 UTC soundings, the CI evaluation failed to detect any differences in the algorithm pairs, see Table 9. This was one of three cases in which the CI method failed. However, upon closer inspection, the CI evaluation of the POTEMP and PIMIX pair was very close to indicating a difference between the two. The upper bound for the interval was .00038, while the lower bound was $-.532$. A shift of only .00039 in the negative direction would have caused the CI evaluation to flag POTEMP and PIMIX as being different. From Table 10, PIMIX had the most number of hits followed by PIMIX day/night, POTEMP and RICH. Although POTEMP had a lower hit rate than either of the PIMIX algorithms, its RMSE was significantly lower compared to the other algorithms. This suggested that POTEMP didn't have as large a variation among its height estimates compared to the PIMIX algorithms, which is understandable considering that it typically produces lower mixed layer heights than does PIMIX (16: Kienzle and Masters 1990).

4.2.2.3 Results for 12 UTC. The Cochran test result for 12 UTC observations indicated that there were differences between the algorithms. From the CI evaluation, RICH differed from both PIMIX day/night and PIMIX; see Table 11. PIMIX accrued the most hits (30) for this test followed by PIMIX day/night, POTEMP and RICH. It was anticipated that PIMIX day/night would have garnered more hits because of its capability to examine shallow, ground-based inversions. However, after reviewing the subjective analyses of the soundings, there were very few cases of ground-based inversions, which partly explains the lower number of hits for PIMIX day/night. The 12 UTC RMSE values listed in Table 12 were generally lower than for 00 UTC, with PIMIX registering the lowest RMSE of all algorithms.

4.2.3 Vandenburg AFB, CA. There were 106 upper air soundings analyzed for Vandenburg AFB, CA, of which 53 were from 00 UTC and 53 were from 12 UTC. Overall algorithm performance was by far the best at this location than of any of

the other four used in the research. Overall, PIMIX day/night registered the most number of hits followed by PIMIX, POTEMP, and RICH.

4.2.3.1 Results for 00 UTC and 12 UTC Combined. The Cochran test yielded $T = 29.58$, which suggested that there were differences in at least two algorithms. Using the CI evaluation, it was determined that RICH differed from both PIMIX and PIMIX day/night; see Table 7. PIMIX day/night logged the most number of hits (79) followed by PIMIX (69), POTEMP (63), and RICH (50). PIMIX day/night had the lowest RMSE, while POTEMP had the highest; see Table 8. Even though RICH obtained the fewest number of hits, it had an RMSE lower than PIMIX and POTEMP, which suggests that RICH has less variability in its height estimates for this location. Ground-based inversions were prevalent in the soundings, which partly explains the lower RMSE values. Also, the sounding profile infrequently indicated deep convective activity. This was evidenced by both the subjective and algorithm height estimates, which were generally less than $3000m$. Since PIMIX day/night had the most hits and the lowest RMSE, it was considered to have the best performance.

4.2.3.2 Results for 00 UTC. Based upon the Cochran test results, there were differences in at least two of the algorithms. The CI evaluation showed that RICH differed from both PIMIX and PIMIX day/night, just as in the 00 UTC and 12 UTC combined test; see Table 9. PIMIX and PIMIX day/night obtained the same number of hits (38) followed by POTEMP (34) and RICH (25). The RMSE values were very low compared to the values for Key West and Lake Charles; see Table 10. PIMIX and PIMIX day/night both had a RMSE of $99m$. RICH had the highest RMSE of $190m$, but even it was less than the lowest RMSE for either Key West or Lake Charles.

4.2.3.3 Results for 12 UTC. From the Cochran test result, at least two of the algorithms were different. Using the CI methodology, RICH was different than both PIMIX and PIMIX day/night; see Table 11. PIMIX day/night logged the most number of hits (41) followed by PIMIX (31), POTEMP (29), and RICH (25). RMSE values for the 12 UTC were larger compared to 00 UTC, with the greatest increases being in the RMSE values for both POTEMP and PIMIX; see Table 12. PIMIX day/night was the best based on the number of hits and low RMSE.

4.2.4 Grand Junction, CO. There were 106 upper air soundings analyzed for Grand Junction, CO, with 53 soundings for both of the 00 UTC and 12 UTC groupings. Algorithm performance for this location was less spectacular than for Vandenburg AFB, but similar to Key West and Lake Charles. Because Grand Junction is located in high mountainous terrain, the upper air soundings were generally very dry due to lack of moisture at higher altitudes. Surprisingly, PIMIX day/night and PIMIX both registered more hits than POTEMP, which was expected to perform well on dry soundings. Additionally, RICH logged more hits than POTEMP for all observation times, unlike the results yielded in Russ' (19: 1999) research.

4.2.4.1 Results for 00 UTC and 12 UTC Combined. Based upon the Cochran test, at least two of the algorithms were different, and the CI evaluation resulted in the following pairs of algorithms being tagged as different: (RICH, PIMIX day/night) and (POTEMP, PIMIX day/night); see Table 7. PIMIX day/night accrued the most hits (46), followed by PIMIX (33), RICH (28), and POTEMP (21). RMSE values were large, especially for POTEMP and PIMIX. PIMIX day/night had the smallest RMSE compared to the other three algorithms; see Table 8. Thus, PIMIX day/night was considered to be the best algorithm for this test.

4.2.4.2 Results for 00 UTC. The Cochran test result indicated that at least two of the algorithms were different. However, the CI evaluation failed to

identify any pairwise differences in the algorithms; see Table 9. The T-value for the test was 13.03, while the critical χ^2 value was 11.35. This was the second case in the research where the CI methodology failed to identify differences in any pair of algorithms. Looking strictly at the number of hits, the algorithms' performances were less than stellar. PIMIX and PIMIX day/night only logged 14 each, RICH had 6 hits, and POTEMP only had 5. However, the RMSE values (except for RICH) were much lower than for the 00 UTC and 12 UTC combined analysis. POTEMP had the lowest RMSE, and RICH had the highest; see Table 10.

4.2.4.3 Results for 12 UTC. The Cochran test for the 12 UTC soundings yielded a T value of 16.23, which was greater than the critical χ^2 value of 11.35. Thus, there were differences in at least two of the algorithms. Employing the CI methodology revealed that the only statistical difference in the number of hits was between POTEMP and PIMIX day/night; see Table 11. POTEMP logged 16 hits, while PIMIX day/night had 32. PIMIX day/night's ground-based inversion logic appeared to be an added strength for this location. PIMIX day/night and RICH had the lowest RMSE values, and there was less variability in the PIMIX day/night RMSE when comparing the 00 UTC and 12 UTC values; see Table 12.

4.2.5 North Platte, NB. There were 103 upper air soundings analyzed for North Platte, NE, with 51 soundings from 00 UTC and 52 from 12 UTC. Both of the PIMIX algorithms had more hits than POTEMP and RICH. PIMIX had the best overall performance, but PIMIX day/night was the better algorithm for the 12 UTC soundings.

4.2.5.1 Results for 00 UTC and 12 UTC Combined. The Cochran test yielded a T value of 17.32, which indicated that there was a difference in at least two of the algorithms. Using the CI evaluation, the following pairs of algorithms were determined to be different: (RICH, PIMIX) and (RICH, PIMIX day/night);

see Table 7. PIMIX recorded 52 hits compared to 49 for PIMIX day/night. Even though RICH had the least number of hits, it had the lowest RMSE of all algorithms followed by PIMIX, PIMIX day/night, and POTEMP; see Table 8.

4.2.5.2 Results for 00 UTC. The T value of 8.4 obtained from the Cochran test for the 00 UTC soundings resulted in no statistical difference in any of the algorithms. PIMIX had the most hits (19) followed by POTEMP (18), PIMIX day/night (15), and RICH (10); see Table 9. POTEMP had the smallest RMSE, while PIMIX day/night had the largest; see Table 10.

4.2.5.3 Results for 12 UTC. Although the Cochran test results suggested a statistical difference between at least two of the algorithms, the CI evaluation failed to identify any pairwise differences in them. This was the last of three cases in this research in which the CI methodology failed. The algorithms were so close to being the same that the CI method could not detect the subtle differences in the number of hits each algorithm logged. PIMIX day/night had 34 hits, while PIMIX had 33. RICH and POTEMP both logged 22 hits each. POTEMP had about the same number of hits for both the 00 UTC and 12 UTC soundings. PIMIX and PIMIX day/night, doubled their hits for 12 UTC compared to 00 UTC; see table 11. The PIMIX algorithms had the lowest RMSE values for 12 UTC, while POTEMP had the highest; see table 12. This was exactly the opposite compared to the 00 UTC portion of the test.

4.3 Forecast Results

In this section, 527 subjective heights obtained from the analyses of RAMS soundings were compared to the RICH, POTEMP, PIMIX, PIMIX-NM1, PIMIX-NM2, and PIMIX day/night algorithm heights. This resulted in 15 pairwise comparisons, as discussed in Chapter 3. The critical χ^2 value was 15.09 for all tests conducted in this portion of the research. Algorithm RMSEs were calculated in the

same manner as for the observed soundings. The numeric results of the statistical analyses of the RAMS forecast soundings are provided in Appendix C.

4.3.1 Key West, FL. There were 107 soundings analyzed for Key West, FL, with 53 soundings from 00 UTC and 54 from 12 UTC. Overall algorithm performance at this location was dismal. Because the RAMS soundings were very smooth as a result of spatial averaging, conducting a subjective analysis of the profile was quite difficult for this location. The subjective heights rarely exceeded $1500m$, even for the summer soundings when convective activity would have been at its peak. The family of PIMIX algorithms consistently returned mixed layer heights of over $9000m$ from late May through early October. That the mixed layer could maintain a height of $9000m$ for several days or weeks is highly unlikely.

4.3.1.1 Results for 00 UTC and 12 UTC Combined. The Cochran test yielded a T value of 26.31, which suggested that there was a difference in at least two of the algorithms. The CI evaluation of the 15 pairs of algorithms revealed that RICH was different from all of the other algorithms; see Table 13. Unexpectedly, RICH registered the most hits (25) for this location, followed by PIMIX-NM2 with 12. The other algorithms had ten or less hits. The RMSE values for all of the various PIMIX algorithms were excessively large, most notably because they frequently returned mixed layer heights of $9000m$ or greater; see Table 16. RICH and POTEMP had comparable RMSE values of $293m$ and $277m$, respectively.

4.3.1.2 Results for 00 UTC. With a T value of 24.08 obtained from the Cochran test, there was a difference in at least two of the algorithms. The CI evaluation flagged the following pairs of algorithms as being different: (RICH, PIMIX), (RICH, PIMIX day/night), and (RICH, PIMIX-NM1); see Table 14. Once again, RICH registered the most hits (15), while the other algorithms each garnered

less than 10 hits each. RICH and POTEMP continued to have comparable RMSE values (267m and 287m, respectively); see Table 17.

4.3.1.3 Results for 12 UTC. Based upon the Cochran test result, there was no statistical difference between any of the algorithms for the 12 UTC soundings; see Table 15. All six of the algorithms had lackluster performances, as they registered 10 or less hits each. RMSE values were comparable to the 12 UTC results; see Table 18, where RICH and POTEMP had the lowest RMSE. The PIMIX algorithms continued to have excessively large RMSE values.

4.3.2 Lake Charles, LA. There were 108 soundings analyzed for Lake Charles, LA, with 54 soundings from both 00 UTC and 12 UTC. Algorithm performance here was markedly better than for Key West. The PIMIX-NM1 and NM2 algorithms garnered the most hits and had their lowest RMSE values for the 12 UTC soundings, suggesting that their strength lies in analyzing early morning soundings. Of course, the fact that these two algorithms were specifically designed to ingest RAMS data, certainly influences their performance compared to the other algorithms.

4.3.2.1 Results for 00 UTC and 12 UTC Combined. The Cochran test for the 00 UTC and 12 UTC soundings combined resulted in a T value of 15.71, which suggested that at least two of the algorithms were different. The CI results indicated that the only two algorithms that differed were RICH and PIMIX-NM2; see Table 13. PIMIX-NM2 registered the most hits (41), while RICH had the fewest (24). RMSE values continued to be large for the PIMIX algorithms. However, PIMIX-NM2 had the smaller RMSE value of all of the PIMIX algorithms. RICH had the smallest RMSE value of all algorithms followed by POTEMP; see Table 16.

4.3.2.2 Results for 00 UTC. There were no differences in any of the algorithms for the 00 UTC soundings based upon the Cochran test result; see

Table 14. PIMIX-NM2 logged the most hits (15), but RICH had the lowest RMSE value; see Table 17. The PIMIX algorithms had very high RMSE values for 00 UTC sounding, similar to those for Key West. Since there the algorithms were statistically the same, PIMIX-NM2 was chosen as the better algorithm since it had the most number of hits.

4.3.2.3 Results for 12 UTC. As was the case for 00 UTC, there were no differences in the algorithms for the 12 UTC soundings. PIMIX-NM2 had the most hits (26), while RICH had the fewest. RICH had the smallest RMSE value, followed by POTEMP. Interestingly, PIMIX-NM1 and PIMIX-NM2 RMSE values were significantly smaller (758m and 738m, respectively) compared to their 00 UTC RMSE values which were in excess of 6200m; see Table 18. Once again, since the algorithms were statistically the same, PIMIX-NM2 was chosen to be better based on the number of hits and RMSE value.

4.3.3 Vandenburg AFB, CA. There were 105 soundings analyzed for Vandenburg AFB, CA, with 52 soundings from 00 UTC and 53 from 12 UTC. Overall algorithm performance (number of hits and RMSE values) for this location was the best compared to the other sites used in the research. It was evident that as the algorithms analyzed drier soundings, they generally registered more hits.

4.3.3.1 Results for 00 UTC and 12 UTC Combined. The Cochran test yielded a T value of 32.78, which suggested that at least two of the algorithms were different. From the CI evaluation, the following pairs of algorithms were determined to be different: (RICH, PIMIX-NM2), (PIMIX day/night, PIMIX-NM2), (PIMIX-NM1, PIMIX-NM2), and (PIMIX, PIMIX-NM2); see Table 13. PIMIX-NM2 registered the most hits (57), while RICH had the fewest (34). PIMIX-NM2 also had the lowest RMSE value (185m), yet the other PIMIX algorithms had RMSE values that exceeded (500m); see Table 16. Because PIMIX-NM2 had the most hits

and the lowest RMSE, it was selected as the best algorithm for the 00 UTC and 12 UTC soundings combined.

4.3.3.2 Results for 00 UTC. With a T value of 55.23, it was determined that there were differences between at least two of the algorithms for the 00 UTC soundings. The CI evaluation results concluded that there were differences in 7 of the 15 algorithm pairs analyzed; see Table 14. PIMIX-NM2 differed from all algorithms except RICH. PIMIX-NM2 had the most number of hits and the smallest RMSE value. RMSE values for all algorithms compared to the 00 UTC and 12 UTC combined soundings; see Table 17. PIMIX-NM2 and POTEMP had similar performances, but PIMIX-NM2 was selected as the best algorithm based upon its RMSE and the number of hits it logged.

4.3.3.3 Results for 12 UTC. The Cochran test result suggested that there were differences between at least two of the algorithms, and based upon the findings of the CI evaluation, it was determined that RICH differed from the other five algorithms; see Table 15. PIMIX-NM1 and NM2 had the same number of hits (37), while RICH had the fewest hits (20) of all algorithms; see Table 18. RMSE values for all algorithms as a whole were the lowest for any location or sounding time evaluated in the research, which may be attributed to the frequent occurrence of ground-based inversions in the 12 UTC soundings. Since the subjective analysis method followed the same logic (default height of $100m$) as the algorithms for ground-based inversions, the RMSE values for those cases would be zero. Thus, those RMSE values would partially mask the larger errors that may have resulted from other than the ground-based inversion cases. RICH had the largest RMSE ($222m$), while PIMIX day/night had the smallest ($143m$). There was no definitive best algorithm for the 12 UTC soundings since RICH was the only distinctly different algorithm and had the fewest hits. Thus, in keeping with the results of the previous tests for this location, PIMIX-NM2 would be the better choice for this location.

4.3.4 Grand Junction, CO. There were 105 soundings analyzed for Grand Junction, CO, with 52 from 00 UTC and 53 from 12 UTC. The algorithms had less difficulty analyzing the 12 UTC soundings, as evidenced by the lower RMSE values compared to the 00 UTC values. PIMIX-NM2 had the most number of hits in each test conducted, and while its RMSE value was large for the 00 UTC soundings, its 12 UTC RMSE was the lowest value recorded in this research.

4.3.4.1 Results for 00 UTC and 12 UTC Combined. For the 00 UTC and 12 UTC soundings combined, the Cochran test yielded a T value of 62.63, which suggested that there was a difference between at least two of the algorithms. The CI evaluation concluded that PIMIX-NM2 was different than any of the other algorithms; see Table 13. PIMIX-NM2 registered more hits (62) than any of the other algorithms. Its closest competitors were PIMIX-NM1 and PIMIX day/night with 42 hits each. POTEMP logged the fewest hits with only 21. RMSE values were quite large for all algorithms except for RICH with an RMSE of 138m; see Table 16. Since RICH will not return a height greater than 4000m, the RICH heights matched fairly well with the predominately low subjective heights for this location. The PIMIX family of algorithms had the largest RMSE values, yet PIMIX-NM2 had the smallest of the group. Although the PIMIX-NM2 RMSE value was large, it had the most number of hits in the analysis, which suggested that when the algorithm was "bad" (did not hit), then it was really bad (had grossly large errors).

4.3.4.2 Results for 00 UTC. With a T value of 42.53 from the Cochran test, at least two of the algorithms were different. The CI evaluation results indicated that the family of PIMIX algorithms were statistically the same. Both RICH and POTEMP differed from each of the PIMIX algorithms; see Table 14. PIMIX-NM2 had the most hits (27) of the family, while the other three algorithms in the family each collected 17. POTEMP had the fewest number of hits with only 2, which was a dismal performance. RMSE values for the 00 UTC soundings were

large, once again; see Table 17. RICH continued to have the lowest RMSE value of 131m.

4.3.4.3 Results for 12 UTC. The Cochran test for the 12 UTC soundings yielded a T value of 24.21, which suggested that at least two of the algorithms were different. Three of the PIMIX algorithms were statistically the same: PIMIX day/night, PIMIX-NM1, and PIMIX-NM2; see Table 15. PIMIX-NM2 logged the most hits with 35, while PIMIX day/night and PIMIX-NM1 garnered 25 hits each. POTEMP had the fewest number of hits with 19. RMSE values dropped dramatically for the PIMIX family of algorithms. PIMIX-NM2 had the smallest RMSE (87m) of all algorithms not only this location and time, but for every other location and time (including the observed section) used in this research; see Table 18. It appeared that the ability of PIMIX-NM2 to avoid skipping over the low-based, shallow inversions enabled it to register more hits than the other algorithms. Furthermore, the occurrence of ground-based inversions also aided in reducing the RMSE values not only for PIMIX-NM2, but for the other algorithms as well. Thus, PIMIX-NM2 was deemed to be the better algorithm for the 12 UTC soundings.

4.3.5 North Platte, NB. There were 102 RAMS soundings analyzed for North Platte, NE, with 50 from 00 UTC and 52 from 12 UTC. As was the case for Grand Junction, the algorithms had greater difficulty analyzing the 00 UTC soundings. PIMIX-NM2 had the most number of hits in each test conducted. However, PIMIX-NM2 had large RMSE values, suggesting that it had great variability among its mixed layer height measurements.

4.3.5.1 Results for 00 UTC and 12 UTC Combined. The Cochran test result ($T = 38.78$) suggested that at least two of the algorithms were different, and the CI evaluation identified differences between the following algorithm pairs: (RICH, PIMIX-NM2), (POTEMP, PIMIX-NM2), and (PIMIX, PIMIX-NM2); see

Table 13. Thus, PIMIX-NM1 and NM2 were statistically the same. PIMIX-NM2 logged 59 hits compared to 46 for PIMIX-NM1. RICH had the fewest hits (32), but had the lowest RMSE value; see Table 16. Each of PIMIX algorithms had RMSE values that exceeded 3000m, which suggests that they frequently get hits, but the error associated with a miss is typically very large.

4.3.5.2 Results for 00 UTC. From the Cochran test's T value of 22.48, at least two of the algorithms were different. Only one algorithm pair was identified as being different as a result of the CI evaluation: (POTEMP, PIMIX-NM2), which made it difficult to select a best algorithm; see Table 14. PIMIX-NM2 registered 22 hits, while POTEMP had only 5. RICH had 12 hits and the smallest RMSE of all the algorithms; see Table 17. PIMIX-NM2 was selected to be the best algorithm based on the number of hits.

4.3.5.3 Results for 12 UTC. With a T value of 29.54 from the Cochran test, it was evident that at least two of the algorithms were different. The CI evaluation identified differences in the following three algorithm pairs: (RICH, PIMIX day/night), (RICH, PIMIX-NM1), (RICH, PIMIX-NM2); see Table 15. PIMIX-NM2 had the most hits (37) followed by PIMIX-NM1 (33), PIMIX day/night (32), POTEMP (29), and RICH (20). The RMSE values for all of the algorithms were lower for the 12 UTC soundings that for 00 UTC; see Table 18. POTEMP had the lowest value of 179m, while both PIMIX-NM1 and NM2 had errors near 2200m, so while those two algorithms may provide more hits, they will typically have gross errors when they miss. This was evident throughout the forecast portion of the research. Therefore, if the number of hits is important, the PIMIX-NM2 is the best algorithm. However, if less error is paramount then POTEMP would be the algorithm of choice for this location.

V. *Conclusions and Recommendations*

5.1 Overview

This chapter is divided into three sections: summary of conclusions, recommendations, and future research opportunities. In the summary of conclusions, the results of the statistical analyses for the observed and forecast portions of the research in Chapter 4 are summarized. The recommendations section provides recommendations for selecting the best algorithm for a particular application. Recommendations for further research are also presented.

5.2 Summary of Conclusions

5.2.1 Observation. In the observed portion of this research, four SLAM algorithms used observed soundings as input and returned mixed layer heights which were then compared to subjective heights obtained from hand-analyses of the observed soundings. The algorithms were subjected to statistical testing to determine if there was any difference in the number of hits they logged for each geographic location used in this research. The research results did not identify a truly "best" algorithm for observed soundings. In all cases, there were at least two algorithms whose hit counts were statistically the same. As a result, the "best" algorithm was identified as having the most number of hits. Table 5 provides a summary of the "best" algorithms for observed soundings based upon location and time. The algorithm(s) with statistically the same number of hits as the "best" are placed in parentheses. Algorithms denoted by an asterisk were selected as the "best" algorithm based on number of hits even though the confidence interval analysis failed to identify statistical differences between any of the four algorithms.

As was the case in Russ' (19: 1999) research, the PIMIX algorithms generally had the better performance (most number of hits) for all locations, but they typically had the largest RMSE values. Therefore, when selecting an algorithm, one must de-

Table 5 Best algorithm for observed soundings based upon location and time.

Time	KEYW	KLCH	KVBG	KGJT	KLBF
00 &12 UTC	PIMIX (PIMIX d/n)	PIMIX (PIMIX d/n)	PIMIX d/n (PIMIX) (POTEMP)	PIMIX d/n (PIMIX)	PIMIX d/n (PIMIX) (POTEMP)
00 UTC	PIMIX (PIMIX d/n)	PIMIX*	PIMIX d/n (PIMIX) (POTEMP)	PIMIX d/n*	PIMIX d/n (All)
12 UTC	PIMIX (PIMIX d/n)	PIMIX (PIMIX d/n) (POTEMP)	PIMIX d/n (PIMIX) (POTEMP)	PIMIX d/n (PIMIX)	PIMIX d/n*

cide whether the number of hits or the amount of error is more important. The new PIMIX day/night algorithm was the "best" algorithm for locations whose regimes were not subject to tropical airmass influences. Table 5 shows that there was no difference in algorithm performance when the statistical analyses were temporally stratified.

5.2.2 Forecast. In the forecast portion of this research, six of the SLAM algorithms ingested RAMS generated soundings and returned mixed layer heights which were then compared to subjective heights obtained from hand-analyses of the RAMS soundings. Because the RAMS soundings were much smoother than observed soundings, determining the subjective mixed layer height was difficult. The subjective heights were much smaller than in the observed portion of the research. Conversely, the PIMIX algorithms tended to return larger mixed layer height measurements for RAMS soundings than for observed soundings. Russ also noted this observation in his research (19: 1999). The research results identified a truly "best" algorithm for two cases using 00 and 12 UTC soundings combined: Key West and Grand Junction. For all other cases, there were at least two algorithms whose hit counts were statistically the same. As a result, the "best" algorithm was identified as having the most number of hits. Table 6 provides a summary of the "best"

algorithms for RAMS soundings based on location and time. The alorithm(s) with statistically the same number of hits as the "best" are placed in parentheses.

Table 6 Best algorithm for RAMS soundings based upon location and time.

Time	KEYW	KLCH	KVBG	KGJT	KLBF
00&12 UTC	RICH	PIMIX-NM2 (All but RICH)	PIMIX-NM2 (POTEMP)	PIMIX-NM2	PIMIX-NM2 (PIMIX-NM1) (PIMIX d/n)
00 UTC	RICH (POTEMP) (PIMIX-NM1)	PIMIX-NM2 (All)	PIMIX-NM2 (RICH)	PIMIX-NM2 (PIMIX-NM1) (PIMIX) (POTEMP)	PIMIX-NM2 (All but RICH)
12 UTC	RICH (All)	PIMIX-NM2 (All)	PIMIX-NM2 (All but RICH)	PIMIX-NM2 (PIMIX-NM1)	PIMIX-NM2 (All but RICH)

The PIMIX-NM2 algorithm proved to be the best algorithm for all locations except Key West, FL, suggesting that a closer inspection of PIMIX-NM2 for tropical soundings is warranted. The selection of the best algorithm was based upon the number of hits. The PIMIX-NM2 algorithm logged the most hits at each location, except Key West, but it typically had the largest RMSE values. Therefore, when selecting an algorithm to analyze RAMS soundings, one must decide whether more hits or less error is more important. Table 6 shows that there was no difference in algorithm performance when the statistical analyses were temporally stratified.

5.3 Recommendations

5.3.1 Selecting an Algorithm. When using observed soundings to determine mixed layer heights, the PIMIX day/night algorithm should be selected for areas that are not influenced by tropical airmasses. For modeling purposes (i.e., using RAMS soundings), PIMIX-NM2 should be the algorithm of choice, especially in drier, continental climates where shallow, low-based inversions are more likely to occur.

5.3.2 Future Research Opportunities. In order to do any further testing and analyses of the SLAM algorithms, the subjective analysis technique used in this research must be automated (i.e., a new algorithm must be created) to facilitate the analyses of larger numbers of soundings. In doing so, the effects of human error and inconsistency can be eliminated, and mixed layer heights can be estimated with more precision than can be afforded by the human eye. Developing an algorithm that analyzes the profile of virtual potential temperature holds promise since moist processes and buoyancy effects are taken directly into account.

If a new virtual potential temperature algorithm were developed, more sophisticated testing could be performed on the SLAM algorithms. It would be of interest to know whether the algorithms perform better than simple random guessing. However, in order to determine that, a much larger data set would need to be analyzed in order to have enough data points to determine the population distribution. Once the population distribution is determined, random height estimates could be generated and statistically compared to the truth heights. Additionally, determining if there is any difference in algorithm performance based upon seasonal stratification could be of use to AFTAC. Once again, this would require a very large data set since there would be four different data sets (one for each season) generated.

Ultimately, comparing the algorithms' mixed layer height estimates to heights obtained from direct-measurement devices such as LIDAR or SODAR would provide the truest evaluation of algorithm performance. It would also provide more meaningful RMSE values which could be used to judge the algorithms' strengths and weaknesses. It is unlikely that, in the near future, this could be done for as many geographic locations used in this research; however, if it could be done for just one location the results would be useful.

Appendix A. Acronyms Used

- AFTAC - Air Force Technical Applications Center
- AGL - Above Ground Level
- ASL - Above Sea Level
- CI - Confidence Interval
- GEMPAK - General Meteorological Package
- LIDAR - Light Detection and Ranging
- N-AWIPS - National Centers Advanced Weather Interactive Processing System
- PBL - Planetary Boundary Layer
- PIMIX - Potential Instability Algorithm
- POTEMP - Potential Instability Algorithm
- RAMS - Regional Atmospheric Modeling System
- RICH - Gradient Richardson Algorithm
- RMSE - Root Mean Square Error
- SLAM - Short Range Layered Atmospheric Model
- SODAR - Sound Detection and Ranging
- USAEDS - United States Atomic Energy Detection System

Appendix B. Statistical Results Using Observed Soundings

B.1 Appendix Organization

This appendix contains the results of the statistical analyses conducted using observed upper air soundings. The results are grouped according to the observation times. The following abbreviations were used in the tables in order to conserve space: Ri is RICH, Po is POTEMP, Pi is PIMIX, and Pd is PIMIX day/night. Each column in the table represents an observation location. Location names were abbreviated as: EY is Key West, LC is Lake Charles, VB is Vandenburg AFB, GJ is Grand Junction, and LB is North Platte. The critical χ^2 value for all tests using observed soundings was 11.35. If, as a result of confidence interval (CI) evaluation, a pair of algorithms was considered to be the same, then the pair was assigned an "S" in the table. Likewise, if the algorithm pair was different, a "D" was entered in the table. If the CI evaluation failed to identify differences in the algorithm pairs, then an "S" in bold type was entered in the table.

Table 7 Results of Cochran tests and CI analyses for all observing sites using 00 UTC and 12 UTC observed soundings combined.

00-12 UTC	EY (58.65)	LC (41.80)	VB (29.58)	GJ (23.03)	LB (17.32)
(Ri,Po)	S	S	S	S	S
(Ri,Pd)	D	D	D	D	D
(Ri,Pi)	D	D	D	S	D
(Po,Pd)	D	S	S	D	S
(Po,Pi)	D	D	S	S	S
(Pd,Pi)	S	S	S	S	S

Table 8 Algorithm hits, hit rates, and RMSE using 00 UTC and 12 UTC observed soundings combined. HR = hit rate.

00-12 UTC	**SITE**	**HITS**	**HR**	**RMSE(m)**
Ri	EY	11	.11	949
Ri	LC	19	.18	1116
Ri	VB	50	.47	205
Ri	GJ	28	.26	646
Ri	LB	32	.31	433
Po	EY	24	.23	734
Po	LC	35	.33	573
Po	VB	63	.59	681
Po	GJ	21	.20	2298
Po	LB	40	.39	976
Pd	EY	45	.43	833
Pd	LC	50	.48	935
Pd	VB	79	.75	131
Pd	GJ	46	.43	630
Pd	LB	49	.48	730
Pi	EY	49	.47	775
Pi	LC	55	.52	669
Pi	VB	69	.65	564
Pi	GJ	33	.31	1398
Pi	LB	52	.51	675

Table 9 Results of Cochran tests and CI analyses for all observing sites using 00 UTC observed soundings.

00 UTC	EY (20.43)	LC (12.43)	VB (17.57)	GJ (13.03)	LB (8.4)
(Ri,Po)	S	**S**	S	**S**	S
(Ri,Pd)	D	**S**	D	**S**	S
(Ri,Pi)	D	**S**	D	**S**	S
(Po,Pd)	S	**S**	S	**S**	S
(Po,Pi)	S	**S**	S	**S**	S
(Pd,Pi)	S	**S**	S	**S**	S

Table 10 Algorithm hits, hit rates, and RMSE using 00 UTC observed soundings. HR = hit rate.

00 UTC	**SITE**	**HITS**	**HR**	**RMSE(m)**
Ri	EY	7	.14	1070
Ri	LC	11	.21	1061
Ri	VB	25	.47	190
Ri	GJ	6	.11	646
Ri	LB	32	.31	575
Po	EY	12	.23	949
Po	LC	10	.37	573
Po	VB	34	.64	101
Po	GJ	5	.01	261
Po	LB	18	.35	189
Pd	EY	21	.41	940
Pd	LC	22	.42	979
Pd	VB	38	.72	99
Pd	GJ	14	.26	412
Pd	LB	15	.29	1026
Pi	EY	21	.41	930
Pi	LC	25	.48	977
Pi	VB	38	.72	99
Pi	GJ	14	.26	412
Pi	LB	19	.37	951

Table 11 Results of Cochran tests and CI analyses for all observing sites using 12 UTC observed soundings.

12 UTC	**EY (39.0)**	**LC (31.77)**	**VB (16.35)**	**GJ (16.23)**	**LB (15.77)**
(Ri,Po)	S	S	S	S	**S**
(Ri,Pd)	D	D	D	S	**S**
(Ri,Pi)	D	D	S	S	**S**
(Po,Pd)	S	S	S	D	**S**
(Po,Pi)	D	S	S	S	**S**
(Pd,Pi)	S	S	S	S	**S**

Table 12 Algorithm hits, hit rates, and RMSE using 12 UTC observed soundings. HR = hit rate.

12 UTC	SITE	HITS	HR	RMSE(m)
Ri	EY	4	.06	802
Ri	LC	8	.15	1005
Ri	VB	25	.47	209
Ri	GJ	22	.42	468
Ri	LB	22	.42	174
Po	EY	12	.23	465
Po	LC	16	.30	741
Po	VB	29	.55	936
Po	GJ	16	.30	2434
Po	LB	22	.42	1380
Pd	EY	24	.45	541
Pd	LC	28	.53	716
Pd	VB	41	.77	151
Pd	GJ	32	.60	623
Pd	LB	34	.65	114
Pi	EY	28	.53	541
Pi	LC	30	.57	210
Pi	VB	31	.59	774
Pi	GJ	19	.36	1466
Pi	LB	33	.64	81

Appendix C. Statistical Results Using RAMS Soundings

C.1 Appendix Organization

This appendix contains the results of the statistical analyses conducted using the RAMS forecast upper air soundings. The results are grouped according to the observation times. The algorithms were abbreviated as follows: Ri is RICH, Po is POTEMP, Pi is PIMIX, Pd is PIMIX day/night, P1 is PIMIX-NM1, and P2 is PIMIX-NM2. Each column in the table represents an observation location. Location names were abbreviated as: EY is Key West, LC is Lake Charles, VB is Vandenburg AFB, GJ is Grand Junction, and LB is North Platte. T values for each location are in parentheses. The critical χ^2 value for all tests using RAMS soundings was 15.09. If a pair of algorithms was considered to be the same, then the pair was assigned an "S" in the table. Likewise, if the algorithm pair was different, a "D" was entered in the table.

Table 13 Results of Cochran tests and CI analyses for all observing sites using 00 and 12 UTC RAMS soundings combined.

00-12 UTC	**EY (26.31)**	**LC (15.71)**	**VB (32.78)**	**GJ (62.63)**	**LB (38.78)**
(Ri,Po)	D	S	S	S	S
(Ri,Pd)	D	S	S	S	S
(Ri,P1)	D	S	S	S	S
(Ri,P2)	D	D	D	D	D
(Ri,Pi)	D	S	S	S	S
(Po,Pd)	S	S	S	D	S
(Po,P1)	S	S	S	D	S
(Po,P2)	S	S	S	D	D
(Po,Pi)	S	S	S	S	S
(Pd,P1)	S	S	S	S	S
(Pd,P2)	S	S	D	D	S
(Pd,Pi)	S	S	S	S	S
(P1,P2)	S	S	D	D	S
(P1,Pi)	S	S	S	S	S
(P2,Pi)	S	S	D	D	D

Table 14 Results of Cochran tests and CI analyses for all observing sites using 00 UTC RAMS soundings.

00 UTC	EY (24.08)	LC (5.65)	VB (55.23)	GJ (45.53)	LB (22.48)
(Ri,Po)	S	S	S	S	S
(Ri,Pd)	D	S	D	S	S
(Ri,P1)	D	S	D	S	S
(Ri,P2)	S	S	S	D	S
(Ri,Pi)	D	S	D	S	S
(Po,Pd)	S	S	S	D	S
(Po,P1)	S	S	S	D	S
(Po,P2)	S	S	D	D	D
(Po,Pi)	S	S	S	D	S
(Pd,P1)	S	S	S	S	S
(Pd,P2)	S	S	D	S	S
(Pd,Pi)	S	S	S	S	S
(P1,P2)	S	S	D	S	S
(P1,Pi)	S	S	S	S	S
(P2,Pi)	S	S	D	S	S

Table 15 Results of Cochran tests and CI analyses for all observing sites using 12 UTC RAMS soundings.

12 UTC	EY (5.53)	LC (13.36)	VB (42.12)	GJ (24.21)	LB (29.59)
(Ri,Po)	S	S	D	S	S
(Ri,Pd)	S	S	D	S	D
(Ri,P1)	S	S	D	S	D
(Ri,P2)	S	S	D	D	D
(Ri,Pi)	S	S	D	S	S
(Po,Pd)	S	S	S	S	S
(Po,P1)	S	S	S	D	S
(Po,P2)	S	S	S	D	S
(Po,Pi)	S	S	S	S	S
(Pd,P1)	S	S	S	S	S
(Pd,P2)	S	S	S	S	S
(Pd,Pi)	S	S	S	S	S
(P1,P2)	S	S	S	S	S
(P1,Pi)	S	S	S	S	S
(P2,Pi)	S	S	S	D	S

Table 16 Algorithm hits, hit rates, and RMSE using 00 and 12 UTC RAMS soundings combined. HR = hit rate.

00-12 UTC	**SITE**	**HITS**	**HR**	**RMSE(m)**
Ri	EY	25	.23	293
Ri	LC	24	.22	279
Ri	VB	34	.32	254
Ri	GJ	35	.33	138
Ri	LB	32	.31	306
Po	EY	10	.09	277
Po	LC	26	.24	316
Po	VB	43	.41	234
Po	GJ	21	.20	1265
Po	LB	34	.33	437
Pd	EY	8	.075	6556
Pd	LC	31	.29	5389
Pd	VB	37	.35	666
Pd	GJ	42	.40	2735
Pd	LB	43	.42	3060
P1	EY	9	.084	6679
P1	LC	32	.30	4573
P1	VB	39	.37	505
P1	GJ	42	.40	2689
P1	LB	46	.45	3665
P2	EY	12	.11	6678
P2	LC	41	.38	4570
P2	VB	57	.54	185
P2	GJ	62	.59	2411
P2	LB	59	.59	3663
Pi	EY	8	.075	6556
Pi	LC	29	.27	5389
Pi	VB	36	.34	670
Pi	GJ	39	.37	2737
Pi	LB	38	.37	3061

Table 17 Algorithm hits, hit rates, and RMSE using 00 UTC RAMS soundings. HR = hit rate.

00 UTC	SITE	HITS	HR	RMSE(m)
Ri	EY	15	.28	267
Ri	LC	11	.20	296
Ri	VB	14	.27	284
Ri	GJ	13	.25	131
Ri	LB	12	.24	387
Po	EY	5	.09	284
Po	LC	8	.15	354
Po	VB	4	.17	287
Po	GJ	2	.04	1907
Po	LB	5	.10	647
Pd	EY	3	.06	6728
Pd	LC	11	.20	6490
Pd	VB	1	.02	946
Pd	GJ	17	.33	4130
Pd	LB	11	.22	4751
P1	EY	4	.08	6904
P1	LC	11	.204	6215
P1	VB	2	.04	701
P1	GJ	17	.33	4060
P1	LB	13	.26	5041
P2	EY	7	.13	6903
P2	LC	15	.28	6213
P2	VB	20	.39	203
P2	GJ	27	.52	3665
P2	LB	22	.44	5039
Pi	EY	3	.06	6728
Pi	LC	10	.19	6490
Pi	VB	1	.02	946
Pi	GJ	17	.33	4130
Pi	LB	11	.22	4751

Table 18 Algorithm hits, hit rates, and RMSE using 12 UTC RAMS soundings. HR = hit rate.

12 UTC	SITE	HITS	HR	RMSE(m)
Ri	EY	10	.19	319
Ri	LC	13	.24	257
Ri	VB	20	.38	222
Ri	GJ	22	.42	143
Ri	LB	20	.39	238
Po	EY	5	.09	269
Po	LC	18	.33	266
Po	VB	34	.64	170
Po	GJ	19	.36	215
Po	LB	29	.56	179
Pd	EY	5	.09	6357
Pd	LC	20	.37	3746
Pd	VB	36	.68	143
Pd	GJ	25	.47	424
Pd	LB	32	.62	184
P1	EY	5	.09	6416
P1	LC	21	.34	6215
P1	VB	37	.70	182
P1	GJ	25	.47	427
P1	LB	33	.64	2199
P2	EY	5	.09	6416
P2	LC	26	.48	738
P2	VB	37	.70	167
P2	GJ	35	.66	87
P2	LB	37	.71	2196
Pi	EY	5	.09	6357
Pi	LC	19	.35	3746
Pi	VB	35	.66	171
Pi	GJ	22	.42	449
Pi	LB	27	.52	212

Appendix D. Mixed Layer Heights For Key West, FL

Table 19 contains the subjective and algorithm mixed layer heights using observed soundings from calendar year 1996. The following abbreviations were used in the table: OBS is the subjective height, RI is RICH, PO is POTEMP, PI d/n is PIMIX day/night, and PI is PIMIX. Heights are reported in meters AGL. Dates with an asterisk represent the easy cases used to calculate the algorithm RMSE.

Table 19 Mixed layer heights for Key West, FL using observed soundings.

Date/Time(UTC)	OBS	RI	PO	PI d/n	PI
10-Jan-00*	494	600	555	555	555
10-Jan-12*	794	400	849	100	100
11-Jan-00	494	1600	643	1175	1175
19-Jan-12	3994	700	1095	100	4014
20-Jan-00*	344	300	401	401	401
20-Jan-12*	344	100	397	100	396
30-Jan-00	1594	900	1153	1759	1759
30-Jan-12*	1544	400	1116	100	1705
31-Jan-00	394	-500	676	3733	3733
08-Feb-12*	1794	1600	815	100	1882
09-Feb-00*	1544	1600	1539	1539	1539
09-Feb-12*	100	100	1450	100	1529
19-Feb-00*	1194	500	725	1286	1286
19-Feb-12*	1044	100	1118	1117	1117
20-Feb-00*	994	400	1037	1036	1036
28-Feb-12*	669	100	714	714	714
29-Feb-00*	369	300	371	370	370
29-Feb-12*	1994	100	1377	1962	1962
10-Mar-00	844	300	1013	100	1012
10-Mar-12	494	400	648	614	614
11-Mar-00*	1194	100	1446	100	1399
19-Mar-12*	2294	-500	2449	2448	2448
20-Mar-00*	1094	1000	1090	1089	1089
20-Mar-12*	1494	900	1579	1578	1578
30-Mar-00	394	-500	563	532	532

Table 19 cont.

Date-Time(UTC)	OBS	RI	PO	PI d/n	PI
30-Mar-12*	494	-500	556	555	555
31-Mar-00*	294	400	353	352	352
08-Apr-12	5000	-500	1800	292	292
09-Apr-00*	100	400	1394	100	1393
09-Apr-12	5000	400	1529	5317	5317
19-Apr-00	844	500	997	100	996
19-Apr-12*	944	1000	956	956	956
20-Apr-00*	1019	1100	1052	100	1051
28-Apr-12	794	-500	1102	1733	1733
29-Apr-00	494	600	553	4370	4370
29-Apr-12	619	800	897	1985	1985
09-May-00	869	700	865	2526	2526
09-May-12	1594	400	1146	1696	1696
10-May-00*	4194	400	689	4110	4110
18-May-12	869	400	1123	6259	6259
19-May-00*	1794	600	725	1867	1867
19-May-12	1044	400	1305	4578	4578
29-May-12	3794	400	508	4105	4105
30-May-00*	819	700	911	4411	4411
07-Jun-12	569	100	751	1775	1775
08-Jun-00	2294	100	1121	2497	2497
08-Jun-12*	594	600	718	776	776
18-Jun-00	5000	400	723	8057	8057
18-Jun-12	5000	400	1784	5460	5460
19-Jun-00	5000	200	966	9134	9134
27-Jun-12	5000	100	834	8098	8098

Table 19 cont.

Date-Time (UTC)	OBS	RI	PO	PI d/n	PI
28-Jun-00	5000	100	1084	4977	4977
28-Jun-12	1144	400	1179	1240	1240
08-Jul-00	844	700	1095	1740	1740
09-Jul-00	5000	400	656	6122	6122
17-Jul-12	5000	900	1132	4108	4108
18-Jul-00	5000	400	690	4379	4379
18-Jul-12	2044	400	1140	2197	2197
28-Jul-00*	1094	400	1216	1216	1216
28-Jul-12	5000	400	786	3798	3798
29-Jul-00	994	200	1148	2227	2227
06-Aug-12	5000	1000	668	12904	12904
07-Aug-00	1594	500	677	1686	1686
07-Aug-12	5000	400	1123	8300	8300
17-Aug-12	5000	600	1066	7767	7767
18-Aug-00*	1044	800	1336	100	7528
26-Aug-12	5000	-500	1064	7878	7878
27-Aug-00	5000	400	589	5895	5895
27-Aug-12	5000	-500	1078	2748	2748
06-Sep-00	794	100	1042	4462	4462
06-Sep-12*	794	100	736	736	736
07-Sep-00	994	400	1036	3406	3406
15-Sep-12*	1244	-500	1294	1293	1293
16-Sep-00	5000	400	409	5853	5853
16-Sep-12	5000	400	845	5509	5509
26-Sep-00	519	600	824	5063	5063
26-Sep-12*	819	-500	942	3017	3017

Table 19 cont.

Date-Time(UTC)	OBS	RI	PO	PI d/n	PI
27-Sep-00	5000	-500	1062	3424	3424
05-Oct-12	5000	400	1072	2524	2524
06-Oct-00	769	-500	1065	100	14832
06-Oct-12	5000	400	391	2964	2964
16-Oct-00	5000	400	1103	5434	5434
16-Oct-12	5000	400	346	5499	5499
17-Oct-00	5000	400	1083	4685	4685
25-Oct-12*	1794	700	1806	1891	1891
26-Oct-00	2394	400	986	100	1771
26-Oct-12*	1544	500	1622	1648	1648
05-Nov-00	869	400	1108	3405	3405
05-Nov-12	494	700	1130	1481	1481
06-Nov-00	444	500	736	4812	4812
14-Nov-12*	1444	400	1099	1515	1515
15-Nov-00	1994	400	1112	100	1884
15-Nov-12	2294	800	403	2354	2354
25-Nov-00*	1544	400	1683	1682	1682
25-Nov-12*	644	900	824	823	823
26-Nov-00	594	400	811	4554	4554
04-Dec-12*	1544	1000	432	1592	1592
05-Dec-00	1494	400	446	1503	1503
05-Dec-12	3094	700	1119	1775	1775
15-Dec-00	1444	400	318	318	318
15-Dec-12	244	400	372	100	338

Table 19 cont.

Date-Time(UTC)	OBS	RI	PO	PI d/n	PI
16-Dec-00*	1269	400	441	1345	1345
24-Dec-12	2394	-500	1585	100	2452
25-Dec-00	844	100	1068	1483	1483
25-Dec-12*	100	-500	-500	120	120

Table 20 contains the subjective and algorithm mixed layer heights using RAMS soundings from calendar year 1996. The following abbreviations were used in the table: OBS is the subjective height, RI is RICH, PO is POTEMP, PD is PIMIX day/night, P1 is PIMIX-NM1, P2 is PIMIX-NM2, and PI is PIMIX. Heights are reported in meters AGL. Dates with an asterisk represent the easy cases used to calculate the algorithm RMSE.

Table 20 Mixed layer heights for Key West using RAMS soundings.

Date-Time(UTC)	OBS	RI	PO	PD	P1	P2	PI
10-Jan-00*	444	200	639	780	780	446	780
10-Jan-12*	469	600	805	805	802	802	805
11-Jan-00*	469	200	686	1013	1013	1013	1013
19-Jan-12	194	100	699	3770	844	844	3770
20-Jan-00*	294	300	472	591	591	289	591
20-Jan-12*	294	300	404	403	403	403	403
30-Jan-00	294	200	1100	3126	3119	3119	3126
30-Jan-12*	294	300	685	3135	3778	3778	3135
31-Jan-00*	444	300	701	3790	3790	3790	3790
08-Feb-12	1444	100	689	2062	2062	2062	2062
09-Feb-00*	294	500	495	1718	1636	1636	1718
09-Feb-12	1469	500	551	1695	1617	1617	1695
19-Feb-00	1119	100	1078	1077	1077	1077	1077
19-Feb-12*	644	200	893	1032	858	858	1032
20-Feb-00*	469	700	1008	1007	1007	1007	1007
28-Feb-12*	644	200	788	787	794	794	787
01-Mar-00	469	300	833	1040	831	831	1040

Table 20 cont.

Date-Time(UTC)	OBS	RI	PO	PD	P1	P2	PI
01-Mar-12	644	200	791	1025	1025	1025	1025
10-Mar-00*	869	900	1049	1048	1048	1048	1048
10-Mar-12*	444	400	629	629	629	629	629
11-Mar-00*	644	300	1105	1105	1105	1105	1105
19-Mar-12	644	1200	540	10025	9800	9800	10025
20-Mar-00*	644	1000	878	993	993	993	993
20-Mar-12*	869	300	1121	1121	1121	1121	1121
30-Mar-00	444	100	712	8798	844	844	8798
30-Mar-12	469	200	618	618	618	618	618
31-Mar-00*	294	400	478	629	629	289	629
08-Apr-12*	169	200	698	7803	844	844	7803
09-Apr-00*	294	200	712	7842	831	446	7842
09-Apr-12*	294	400	704	5634	5630	5630	5634
19-Apr-00*	869	100	994	993	993	993	993
19-Apr-12*	869	300	1008	1008	1008	1008	1008
20-Apr-00*	894	500	998	997	997	997	997
28-Apr-12	894	200	1085	8818	8818	8818	8818
29-Apr-00*	469	500	681	8797	8797	8797	8797
29-Apr-12*	644	900	903	1078	1078	1078	1078
09-May-00*	869	700	1083	2536	2536	2536	2536
09-May-12*	844	400	908	10152	9842	9842	10152
10-May-00*	644	700	871	10147	9845	9845	10147
18-May-12*	869	600	1119	6651	6651	6651	6651
19-May-00*	494	300	675	4641	4641	4641	4641
19-May-12*	644	700	705	4626	4626	4626	4626
29-May-12	644	400	697	6616	6616	6616	6616

Table 20 cont.

Date-Time(UTC)	OBS	RI	PO	PD	P1	P2	PI
30-May-00	644	200	861	6617	6617	6617	6617
07-Jun-12*	644	300	860	8797	8797	8797	8797
08-Jun-00*	644	300	1084	10006	9731	9731	10006
08-Jun-12*	644	400	897	8782	8782	8782	8782
18-Jun-00	869	300	1053	10110	9821	9821	10110
18-Jun-12*	644	200	831	8781	8781	8781	8781
19-Jun-00*	444	500	691	10128	9835	9835	10128
27-Jun-12	644	300	815	6170	11746	11746	6170
28-Jun-00*	644	500	861	11783	10923	10923	11783
28-Jun-12*	869	300	1140	11847	11847	11847	11847
08-Jul-00	644	500	693	6623	6623	6623	6623
08-Jul-12	469	300	839	11934	10931	10931	11934
09-Jul-00	444	400	892	10943	10893	10893	10943
17-Jul-12	5000	1000	1150	11936	10927	10927	11936
18-Jul-00*	644	1000	838	10246	10867	10867	10246
18-Jul-12*	869	500	1101	10936	10899	10899	10936
28-Jul-00	1144	1200	1403	10183	9820	9820	10183
28-Jul-12*	644	1000	820	10192	9821	9821	10192
29-Jul-00*	644	300	872	10219	10782	10782	10219
06-Aug-12	5000	1200	689	12799	12698	12698	12799
07-Aug-00*	894	900	826	11937	11937	11937	11937
07-Aug-12*	869	400	879	10191	9844	9844	10191
17-Aug-00	894	400	1122	10180	9841	9841	10180
17-Aug-12*	869	600	1106	10200	10864	10864	10200
18-Aug-00*	644	400	880	10919	10900	10900	10919
26-Aug-12	5000	100	1121	12020	10964	10964	12020

Table 20 cont.

Date-Time(UTC)	OBS	RI	PO	PD	P1	P2	PI
27-Aug-00	644	300	918	11973	11973	11973	11973
27-Aug-12	644	500	708	11936	11936	11936	11936
06-Sep-00	669	300	1034	10114	9778	9778	10114
06-Sep-12*	494	300	847	10143	9798	9798	10143
07-Sep-00*	644	100	1082	10143	10847	10847	10143
15-Sep-12	5000	200	1414	6623	6623	6623	6623
16-Sep-00*	444	400	722	11911	11911	11911	11911
16-Sep-12*	444	400	683	6151	11898	11898	6151
26-Sep-00	644	400	1056	10890	10864	10864	10890
26-Sep-12*	869	500	1084	10186	10841	10841	10186
27-Sep-00*	644	400	860	3429	10823	10823	3429
05-Oct-12	5000	100	898	11939	11939	11939	11939
06-Oct-00*	644	300	1107	11849	11849	11849	11849
06-Oct-12*	644	400	894	6611	6611	6611	6611
16-Oct-00	5000	1000	1070	8697	8697	8697	8697
16-Oct-12*	294	400	893	1026	1026	1026	1026
17-Oct-00*	644	700	904	10099	9763	9763	10099
25-Oct-12	1819	900	843	1962	1962	1962	1962
26-Oct-00*	644	900	879	1774	1677	1677	1774
26-Oct-12	1494	900	1124	1719	1602	1602	1719
05-Nov-00	5000	900	1123	11824	10959	10959	11824
05-Nov-12*	744	700	877	11873	10964	10964	11873
06-Nov-00*	494	400	909	11845	10929	10929	11845
14-Nov-12	5000	1000	810	1068	1068	1068	1068
15-Nov-00*	694	1000	1106	7876	7690	7690	7876
15-Nov-12*	494	800	695	1091	1091	1091	1091

Table 20 cont.

Date-Time (UTC)	OBS	RI	PO	PD	P1	P2	PI
25-Nov-00*	1494	1200	1581	1657	1579	1579	1657
25-Nov-12*	644	700	859	1773	1685	1685	1773
26-Nov-00*	469	500	893	6126	10779	10779	6126
04-Dec-12	319	400	687	1079	1079	1079	1079
05-Dec-00	294	500	541	1092	1092	1092	1092
05-Dec-12*	844	400	1119	1772	1677	1677	1772
15-Dec-00	744	100	879	1748	1676	1676	1748
15-Dec-12*	169	400	431	1077	1077	1077	1077
16-Dec-00*	494	500	707	1334	1334	1334	1334
24-Dec-12	5000	200	699	2478	2478	2478	2478
25-Dec-00*	444	200	540	2040	2040	2040	2040
25-Dec-12	144	400	566	1091	1091	1091	1091

Appendix E. Mixed Layer Heights For Lake Charles, LA

Table 21 contains the subjective and algorithm mixed layer heights using observed soundings from calendar year 1996. The following abbreviations were used in the table: OBS is the subjective height, RI is RICH, PO is POTEMP, PI d/n is PIMIX day/night, and PI is PIMIX. Heights are reported in meters AGL. Dates with an asterisk represent the easy cases used to calculate the algorithm RMSE.

Table 21 Mixed layer heights for Lake Charles using observed soundings.

Date/Time (UTC)	OBS	RICH	POTEMP	PIMIX d/n	PIMIX
10-Jan-00*	1140	400	1164	1163	1163
10-Jan-12*	1065	-500	1178	100	1153
11-Jan-00*	1690	400	1705	1705	1705
19-Jan-12*	565	600	639	639	639
20-Jan-00*	815	900	893	100	893
20-Jan-12	1190	400	1444	100	32326
30-Jan-00*	3040	-500	392	3051	3051
30-Jan-12*	2090	1300	2185	100	2250
31-Jan-00*	115	400	226	225	225
08-Feb-12*	100	-500	788	100	100
09-Feb-12	100	-500	1863	100	1895
19-Feb-00*	2365	-500	987	2387	2387
19-Feb-12*	1890	800	1019	100	1984
20-Feb-00*	100	-500	100	100	100
28-Feb-12*	540	600	387	607	607
29-Feb-00*	440	-500	491	491	491
29-Feb-12*	590	600	638	637	637
10-Mar-00*	1240	1000	1305	1305	1305
10-Mar-12*	1490	800	1552	100	1552
11-Mar-00*	1740	-500	1831	1830	1830
19-Mar-12	1540	-500	1759	100	1758
20-Mar-00	790	-500	3170	3169	3169
20-Mar-12*	1190	400	1320	1320	1320
30-Mar-00	1040	-500	1055	1328	1328

Table 21 cont.

Date-Time (UTC)	OBS	RI	PO	PI d/n	PI
30-Mar-12	140	400	281	100	281
31-Mar-00*	1740	100	333	1783	1783
08-Apr-12*	100	-500	100	100	100
09-Apr-00	215	200	376	375	375
09-Apr-12*	100	100	100	100	100
19-Apr-00*	1340	400	626	1443	1443
19-Apr-12*	1240	400	384	1289	1289
20-Apr-00*	765	800	799	799	799
28-Apr-12*	540	400	556	570	570
29-Apr-00*	790	700	884	913	913
29-Apr-12	4290	400	2049	4293	4293
09-May-00*	1890	700	873	1994	1994
09-May-12	2165	400	1115	1070	1070
10-May-00	590	600	643	3910	3910
18-May-12*	640	400	723	711	711
19-May-00	1090	900	1290	1390	1390
19-May-12*	940	400	1027	1095	1095
29-May-12*	690	400	795	843	843
30-May-00*	415	500	493	492	492
07-Jun-12	990	100	1008	3519	3519
08-Jun-00	5000	300	336	4268	4268
08-Jun-12	1940	400	100	100	100
18-Jun-00	3090	900	1104	3135	3135
18-Jun-12	790	100	1210	1183	1183
19-Jun-00	3590	-500	2529	3625	3625
27-Jun-12	5000	100	-500	3098	3098

Table 21 cont.

Date-Time (UTC)	OBS	RI	PO	PI d/n	PI
28-Jun-00	5000	200	428	8582	8582
28-Jun-12*	3390	200	1460	3409	3409
08-Jul-00	5000	400	1297	3991	3991
09-Jul-00	390	400	599	5718	5718
17-Jul-12	5000	100	1098	8891	8891
18-Jul-00	5000	-500	589	5378	5378
18-Jul-12	1090	900	1435	3126	3126
28-Jul-00*	690	400	857	4903	4903
28-Jul-12	840	100	1025	1372	1372
29-Jul-00	5000	400	2257	4727	4727
06-Aug-12	5000	100	868	7860	7860
07-Aug-00	5000	300	381	11674	11674
07-Aug-12	5000	400	903	5921	5921
17-Aug-00*	3990	400	4006	4006	4006
17-Aug-12	5000	100	995	10040	10040
18-Aug-00*	865	1300	1021	1020	1020
26-Aug-12	5000	400	844	3742	3742
27-Aug-00	840	800	868	4173	4173
27-Aug-12	5000	-500	2498	5017	5017
06-Sep-00	2490	-500	2724	3332	3332
06-Sep-12	5000	1000	2668	10663	10663
07-Sep-00	5000	400	1058	5437	5437
15-Sep-12	5000	400	1139	5302	5302
16-Sep-00	740	900	979	2315	2315
16-Sep-12*	1490	500	1555	1586	1586
26-Sep-00	1340	1000	1508	2668	2668

Table 21 cont.

Date-Time (UTC)	OBS	RI	PO	PI d/n	PI
26-Sep-12	100	100	1137	100	1136
27-Sep-00	840	700	949	3633	3633
05-Oct-12	465	500	632	632	632
06-Oct-00	815	400	899	899	899
06-Oct-12	390	400	359	359	359
16-Oct-00	1390	100	1433	100	1447
16-Oct-12	100	100	993	100	992
17-Oct-00	2040	400	721	1330	1330
25-Oct-12*	100	400	100	100	100
26-Oct-00	5000	-500	100	100	962
26-Oct-12*	1440	400	3370	100	1497
05-Nov-00*	1715	400	1740	1740	1740
05-Nov-12*	1940	1000	1101	100	1056
06-Nov-00	1940	400	1102	1468	1468
14-Nov-12	1590	100	1648	100	3618
15-Nov-00	1040	400	1195	100	1701
15-Nov-12*	1840	400	923	100	1882
25-Nov-00	5000	100	1928	100	2925
25-Nov-12*	940	700	1011	1010	1010
26-Nov-00*	915	500	961	961	961
04-Dec-12*	100	1300	1182	100	100
05-Dec-00*	390	400	-500	100	459
05-Dec-12*	100	400	100	100	100
15-Dec-00*	765	700	819	1878	1878

Table 21 cont.

Date-Time (UTC)	OBS	RI	PO	PI d/n	PI
15-Dec-12	1440	400	-500	282	282
16-Dec-00*	915	1000	416	989	989
24-Dec-12*	290	1300	311	100	310
25-Dec-00*	690	1000	826	826	826
25-Dec-12*	100	300	298	100	100

Table 22 contains the subjective and algorithm mixed layer heights using RAMS soundings from calendar year 1996. The following abbreviations were used in the table: OBS is the subjective height, RI is RICH, PO is POTEMP, PD is PIMIX day/night, P1 is PIMIX-NM1, P2 is PIMIX-NM2, and PI is PIMIX. Heights are reported in meters AGL. Dates with an asterisk represent the "easy" cases used to calculate the algorithm RMSE.

Table 22 Mixed layer heights for Lake Charles using RAMS soundings.

Date-Time (UTC)	OBS	RI	PO	PD	P1	P2	PI
10-Jan-00	1140	900	714	997	843	843	997
10-Jan-12*	100	100	100	100	100	100	100
11-Jan-00	100	300	420	100	100	100	1025
19-Jan-12*	640	900	666	740	739	447	740
20-Jan-00*	615	100	667	739	740	447	739
20-Jan-12*	100	300	299	100	100	100	100
30-Jan-00	615	100	891	1104	845	845	1104
30-Jan-12	290	600	477	618	618	289	618
31-Jan-00	190	600	568	1326	1326	1326	1326
08-Feb-12*	100	100	100	100	100	100	100
09-Feb-00*	100	300	100	100	100	100	100
09-Feb-12*	100	300	100	100	100	100	100
19-Feb-00	2340	1300	890	1103	1103	1103	1103
19-Feb-12*	100	900	226	628	100	100	628
20-Feb-00*	190	300	332	441	441	157	441
28-Feb-12	640	100	511	591	591	591	591
01-Mar-00	665	700	732	731	731	731	731

Table 22 cont.

Date-Time (UTC)	OBS	RI	PO	PD	P1	P2	PI
01-Mar-12	290	400	467	562	562	289	562
10-Mar-00*	1140	1200	1284	1284	1284	1284	1284
10-Mar-12*	100	100	734	100	100	100	100
11-Mar-00*	1140	400	1418	1417	1417	1417	1417
19-Mar-12	5000	-500	714	1118	843	289	1118
20-Mar-00	1840	-500	2624	3197	3077	3077	3197
20-Mar-12	100	300	928	100	100	100	1434
30-Mar-00*	790	200	884	1048	1048	1048	1048
30-Mar-12	100	300	100	100	100	100	1007
31-Mar-00*	440	400	655	8883	831	447	8883
08-Apr-12*	100	100	100	100	100	100	100
09-Apr-00*	290	300	562	1078	857	289	1078
09-Apr-12*	100	100	100	100	100	100	100
19-Apr-00	490	700	728	1280	1280	1280	1280
19-Apr-12*	290	600	490	584	584	289	584
20-Apr-00*	640	600	629	629	629	629	629
28-Apr-12*	465	1000	584	584	584	584	584
29-Apr-00*	440	800	652	1019	802	447	1019
29-Apr-12	5000	1200	540	1079	857	857	1079
09-May-00	1890	800	921	2084	2084	2084	2084
09-May-12	5000	600	876	8816	8816	8816	8816
10-May-00*	640	700	859	10081	9842	9842	10081
18-May-12*	615	100	402	768	769	769	768
19-May-00*	615	400	916	8778	8778	8778	8778
19-May-12	5000	900	900	1067	858	858	1067
29-May-00	440	300	694	11905	10929	10929	11905

Table 22 cont.

Date-Time (UTC)	OBS	RI	PO	PD	P1	P2	PI
29-May-12	640	400	662	788	781	781	788
30-May-00*	465	500	600	600	600	600	600
07-Jun-12	5000	100	902	1078	858	858	1078
08-Jun-00*	440	800	717	8800	8800	8800	8800
08-Jun-12*	190	300	704	8817	831	447	8817
18-Jun-00	5000	100	340	10940	10931	10931	10940
18-Jun-12*	190	300	712	11795	832	832	11795
19-Jun-00*	465	800	698	11797	11797	11797	11797
27-Jun-12*	190	200	431	795	795	447	795
28-Jun-00*	465	800	1681	8678	8678	8678	8678
28-Jun-12*	290	500	725	7915	845	845	7915
08-Jul-00	5000	100	386	6585	6585	6585	6585
08-Jul-12	490	700	903	1079	1079	1079	1079
09-Jul-00	5000	1300	836	10137	832	832	10137
17-Jul-12	190	100	521	6215	9799	9799	6215
18-Jul-00	890	400	1106	10913	10874	10874	10913
18-Jul-12	290	400	543	10915	10863	10863	10915
28-Jul-00*	640	400	1392	4631	4631	4631	4631
28-Jul-12	290	400	898	10938	10933	10933	10938
29-Jul-00*	640	500	819	11745	11745	11745	11745
06-Aug-12	5000	100	398	11823	11823	11823	11823
07-Aug-00*	890	700	1086	11847	10896	10896	11847
07-Aug-12*	290	400	728	847	845	845	847
17-Aug-00	490	200	1074	3787	3787	3787	3787
17-Aug-12*	190	200	436	3795	3795	3795	3795

Table 22 cont.

Date-Time (UTC)	OBS	RI	PO	PD	P1	P2	PI
18-Aug-00*	690	1200	1121	10174	9844	9844	10174
26-Aug-12	5000	200	710	804	803	803	804
27-Aug-00*	440	800	708	11932	11932	11932	11932
27-Aug-12	490	500	710	11896	11896	11896	11896
06-Sep-00	5000	100	2147	4630	4630	4630	4630
06-Sep-12*	190	200	705	10053	857	857	10053
07-Sep-00*	465	800	676	10045	9763	9763	10045
15-Sep-12	5000	1000	425	1057	844	844	1057
16-Sep-00*	665	900	893	10888	10865	10865	10888
16-Sep-12	465	900	699	3786	845	845	3786
26-Sep-00	5000	100	1091	11901	10925	10925	11901
26-Sep-12	5000	900	532	11783	10923	10923	11783
27-Sep-00*	465	800	686	11906	11906	11906	11906
05-Oct-12	590	1000	662	796	795	447	796
06-Oct-00	465	600	497	608	608	289	608
06-Oct-12*	415	500	452	557	557	289	557
16-Oct-00	1440	100	1091	1362	1362	1362	1362
16-Oct-12*	100	400	100	100	100	100	100
17-Oct-00*	640	500	903	1090	858	858	1090
25-Oct-12	290	1200	484	599	599	289	599
26-Oct-00*	465	600	618	618	618	618	618
26-Oct-12	640	400	653	100	100	100	738
05-Nov-00	1490	100	691	1651	1572	1572	1651
05-Nov-12	100	300	100	100	100	100	100
06-Nov-00*	290	400	743	1771	1695	1695	1771

Table 22 cont.

Date-Time (UTC)	OBS	RI	PO	PD	P1	P2	PI
14-Nov-12	100	100	100	608	608	157	608
15-Nov-00	490	400	910	1777	1676	1676	1777
15-Nov-12*	100	300	100	100	100	100	100
25-Nov-00	5000	1600	444	1078	811	447	1078
25-Nov-12*	465	500	651	997	780	447	997
26-Nov-00*	890	900	945	945	945	945	945
04-Dec-12	100	400	385	608	608	289	608
05-Dec-00	440	400	618	617	617	617	617
05-Dec-12*	100	300	100	100	100	100	100
15-Dec-00*	640	400	796	795	794	794	795
15-Dec-12*	100	300	100	100	100	100	100
16-Dec-00*	440	400	1119	1326	1326	1326	1326
24-Dec-12*	290	400	433	433	433	433	433
25-Dec-00*	665	400	733	732	734	734	732
25-Dec-12*	100	300	100	100	100	100	100

Appendix F. Mixed Layer Heights For Vandenburg AFB, CA

Table 23 contains the subjective and algorithm mixed layer heights using observed soundings from calendar year 1996. The following abbreviations were used in the table: OBS is the subjective height, RI is RICH, PO is POTEMP, PI d/n is PIMIX day/night, and PI is PIMIX. Heights are reported in meters AGL. Dates with an asterisk represent the easy cases used to calculate the algorithm RMSE.

Table 23 Mixed layer heights for Vandenburg AFB using observed soundings.

Date/Time (UTC)	OBS	RI	PO	PI d/n	PI
10-Jan-00*	463	500	511	511	511
10-Jan-12	138	500	176	100	175
11-Jan-00	313	500	545	2103	2103
19-Jan-12	788	600	873	872	872
20-Jan-00*	313	600	576	575	575
20-Jan-12	100	200	-500	100	1386
30-Jan-00	188	300	290	892	892
30-Jan-12	3438	100	913	100	2371
31-Jan-00	388	300	468	587	587
08-Feb-12*	100	100	3505	100	100
09-Feb-00*	138	200	178	195	195
09-Feb-12*	313	400	370	369	369
19-Feb-00*	88	300	134	133	133
19-Feb-12	1788	300	1919	1919	1919
20-Feb-00	5000	1600	607	1618	1618
28-Feb-12*	100	100	1906	100	1927
29-Feb-00	2488	500	2107	2487	2487
29-Feb-12*	100	-500	2068	100	2068
10-Mar-00*	388	400	413	412	412
10-Mar-12*	100	100	553	100	1700
11-Mar-00	313	400	599	551	551
19-Mar-12	238	300	290	289	289
20-Mar-00	163	200	196	196	196
20-Mar-12*	100	100	46	46	46
30-Mar-00*	338	400	363	377	377

Table 23 cont.

Date-Time (UTC)	OBS	RI	PO	PI d/n	PI
30-Mar-12	100	400	365	100	364
31-Mar-00*	513	200	614	677	677
09-Apr-00*	563	600	606	605	605
09-Apr-12*	938	600	996	100	1029
19-Apr-00*	463	900	562	561	561
19-Apr-12	100	300	1533	100	1532
20-Apr-00*	388	700	256	481	481
28-Apr-12*	100	100	100	100	100
29-Apr-00*	138	200	155	163	163
29-Apr-12*	100	200	100	100	100
09-May-00	238	300	259	312	312
09-May-12	238	300	250	250	250
10-May-00*	288	300	304	303	303
18-May-12*	100	1000	999	100	999
19-May-00	863	200	211	249	249
19-May-12	5000	300	280	1085	1085
29-May-00*	588	-500	-500	-500	-500
29-May-12*	938	1000	951	951	951
30-May-00*	738	500	761	763	763
07-Jun-12*	100	100	100	100	100
08-Jun-00*	288	100	339	347	347
08-Jun-12	100	300	179	180	180
18-Jun-00*	100	-500	-500	100	100
18-Jun-12	1488	200	100	100	100
19-Jun-00	188	300	201	200	200
27-Jun-12	100	100	617	100	924

Table 23 cont.

Date-Time (UTC)	OBS	RI	PO	PI d/n	PI
28-Jun-00*	388	400	526	526	526
28-Jun-12	263	300	249	248	248
08-Jul-00*	738	400	345	345	345
08-Jul-12*	288	400	335	334	334
09-Jul-00*	313	400	338	340	340
17-Jul-12	488	100	506	100	528
18-Jul-00*	438	500	452	451	451
18-Jul-12*	100	400	100	100	100
28-Jul-00*	263	-500	278	277	277
28-Jul-12	238	100	247	100	247
29-Jul-00*	188	200	189	188	188
06-Aug-12	838	200	603	602	602
07-Aug-00*	463	500	528	528	528
07-Aug-12*	488	100	275	538	538
17-Aug-12*	288	100	295	294	294
18-Aug-00*	313	400	337	339	339
26-Aug-12	738	300	523	522	522
27-Aug-00*	163	500	212	211	211
27-Aug-12*	138	200	158	157	157
06-Sep-00*	238	300	256	256	256
06-Sep-12*	100	200	100	100	100
07-Sep-00	100	100	642	619	619
15-Sep-12	1188	400	-500	847	847
16-Sep-00*	213	300	-500	304	304
16-Sep-12*	100	300	679	100	729

Table 23 cont.

Date-Time (UTC)	OBS	RI	PO	PI d/n	PI
26-Sep-00*	563	300	582	589	589
26-Sep-12*	538	300	575	574	574
27-Sep-00*	388	400	420	419	419
05-Oct-12*	100	100	100	100	100
06-Oct-00*	100	100	100	100	100
06-Oct-12*	100	100	100	100	100
16-Oct-00*	38	200	74	73	73
16-Oct-12	138	200	100	100	100
17-Oct-00	100	200	1242	100	100
25-Oct-12	100	300	767	100	1116
26-Oct-00*	788	600	935	935	935
26-Oct-12	100	-500	1479	100	1711
05-Nov-00*	538	800	681	786	786
05-Nov-12	938	300	957	100	957
06-Nov-00*	263	300	343	330	330
14-Nov-12*	213	300	257	256	256
15-Nov-00*	163	600	237	236	236
15-Nov-12	513	300	561	560	560
25-Nov-00*	88	200	125	124	124
25-Nov-12*	100	300	210	100	210
26-Nov-00*	138	300	181	181	181
04-Dec-12*	288	300	353	100	384
05-Dec-00*	88	200	153	153	153
05-Dec-12*	100	100	1411	100	1393
15-Dec-00*	188	300	284	284	284

Table 23 cont.

Date-Time (UTC)	OBS	RI	PO	PI d/n	PI
15-Dec-12*	100	200	2903	100	2857
16-Dec-00*	100	100	100	100	100
24-Dec-12*	100	100	100	100	100
25-Dec-00	88	300	171	671	671
25-Dec-12*	100	100	270	100	269

Table 24 contains the subjective and algorithm mixed layer heights using RAMS soundings from calendar year 1996. The following abbreviations were used in the table: OBS is the subjective height, RI is RICH, PO is POTEMP, PD is PIMIX day/night, P1 is PIMIX-NM1, P2 is PIMIX-NM2, and PI is PIMIX. Heights are reported in meters AGL. Dates with an asterisk represent the easy cases used to calculate the algorithm RMSE.

Table 24 Mixed layer heights for Vandenburg AFB using RAMS soundings.

Date-Time (UTC)	OBS	RI	PO	PD	P1	P2	PI
10-Jan-00*	388	100	570	570	570	570	570
10-Jan-12*	100	300	100	100	100	100	100
11-Jan-00	213	300	481	2064	840	288	2064
19-Jan-12	5000	100	350	1100	1100	634	1100
20-Jan-00*	1438	500	1112	1699	1699	1699	1699
20-Jan-12*	100	300	100	100	100	100	100
30-Jan-00*	588	200	769	1021	766	766	1021
30-Jan-12*	100	300	100	100	100	100	100
31-Jan-00*	413	600	652	1116	828	445	1116
08-Feb-12*	100	100	100	100	100	100	100
09-Feb-00	5000	300	332	415	415	156	415
09-Feb-12*	100	300	100	100	100	100	100
19-Feb-00	488	100	518	4671	791	445	4671
19-Feb-12	5000	400	695	1102	854	854	1102
20-Feb-00	5000	400	304	3239	3160	3160	3239
28-Feb-12*	100	100	100	100	100	100	100
01-Mar-00	388	500	1713	2608	2608	2608	2608

Table 24 cont.

Date-Time (UTC)	OBS	RI	PO	PD	P1	P2	PI
01-Mar-12	100	800	-500	100	100	100	100
10-Mar-00*	238	100	712	1074	817	817	1074
10-Mar-12*	100	200	100	100	100	100	100
11-Mar-00*	238	400	724	1101	828	445	1101
19-Mar-12	100	100	100	100	100	100	100
20-Mar-00	213	200	326	397	397	156	397
20-Mar-12*	100	100	100	100	100	100	100
30-Mar-00	538	100	705	1029	828	828	1029
30-Mar-12*	100	300	100	100	100	100	100
31-Mar-00*	238	500	471	597	597	288	597
08-Apr-12*	100	100	239	397	100	100	397
09-Apr-00*	238	200	471	597	597	288	597
09-Apr-12*	100	100	100	100	100	100	100
19-Apr-00	638	700	853	4710	4710	4710	4710
19-Apr-12*	100	400	100	100	100	100	100
20-Apr-00*	388	400	698	3308	3161	445	3308
28-Apr-12*	100	100	100	100	100	100	100
29-Apr-00	5000	200	295	384	384	156	384
29-Apr-12	39	100	100	100	100	100	100
09-May-00	563	100	669	1036	791	791	1036
09-May-12	100	400	100	100	100	100	100
10-May-00	100	700	338	431	431	156	431
18-May-12	5000	100	426	985	818	288	985
19-May-00	388	400	881	1054	1054	1054	1054
19-May-12	5000	600	100	100	100	100	1028

Table 24 cont.

Date-Time (UTC)	OBS	RI	PO	PD	P1	P2	PI
29-May-00	100	100	100	100	100	100	100
29-May-12*	788	400	100	100	100	100	100
30-May-00	238	300	531	978	784	445	978
07-Jun-12	100	100	100	392	100	100	392
08-Jun-00*	238	500	339	380	380	380	380
08-Jun-12*	100	200	100	100	100	100	100
18-Jun-00	5000	100	351	440	440	156	440
18-Jun-12*	100	400	100	100	100	100	100
19-Jun-00*	100	300	281	280	280	280	280
27-Jun-12*	100	100	398	100	615	156	615
28-Jun-00*	263	500	700	3290	855	855	3290
28-Jun-12*	100	400	100	100	100	100	100
17-Jul-12*	588	100	480	559	559	288	559
18-Jul-00*	238	700	450	559	559	288	559
18-Jul-12*	100	300	100	273	273	273	273
28-Jul-00*	238	400	403	402	402	402	402
28-Jul-12*	100	100	100	100	100	100	100
29-Jul-00*	238	700	380	380	380	380	380
06-Aug-12	738	200	503	575	575	575	575
07-Aug-00*	388	700	461	537	537	288	537
07-Aug-12*	100	300	100	100	100	100	100
17-Aug-00*	100	100	100	392	100	100	392
17-Aug-12*	100	300	100	100	100	100	100
18-Aug-00*	213	400	336	376	376	376	376
26-Aug-12*	588	100	269	423	100	100	423
27-Aug-00*	238	300	441	440	440	440	440

Table 24 cont.

Date-Time (UTC)	OBS	RI	PO	PD	P1	P2	PI
27-Aug-12	100	400	100	100	100	100	100
06-Sep-00	488	100	483	606	606	288	606
06-Sep-12	100	300	100	100	100	100	100
07-Sep-00	238	800	361	440	440	440	440
15-Sep-12	538	100	393	589	589	288	589
16-Sep-00	538	400	565	1015	799	799	1015
16-Sep-12	5000	500	251	251	251	251	251
26-Sep-00*	388	200	534	534	534	534	534
26-Sep-12	100	300	100	100	100	100	100
27-Sep-00*	238	500	416	415	415	415	415
05-Oct-12*	100	100	100	100	100	100	100
06-Oct-00	238	100	323	388	388	156	388
06-Oct-12	100	100	100	100	100	100	100
16-Oct-00*	100	200	256	409	409	156	409
16-Oct-12*	100	400	100	100	100	100	100
17-Oct-00*	100	500	309	431	431	156	431
25-Oct-12	5000	100	442	1009	791	445	1009
26-Oct-00*	588	700	1079	2127	2127	860	2127
26-Oct-12	388	800	723	100	1722	634	1722
05-Nov-00	538	300	537	1009	828	828	1009
05-Nov-12*	100	400	531	100	100	100	100
06-Nov-00*	100	300	888	1100	1100	156	1100
14-Nov-12	238	400	450	582	582	288	582
15-Nov-00*	100	300	332	1036	808	156	1036
15-Nov-12*	238	600	431	100	431	431	431

Table 24 cont.

Date-Time (UTC)	OBS	RI	PO	PD	P1	P2	PI
25-Nov-00*	100	100	333	589	589	156	589
25-Nov-12*	100	100	100	100	100	100	100
26-Nov-00*	100	300	100	1101	828	288	1101
04-Dec-12	238	200	337	408	100	100	408
05-Dec-00	5000	300	704	1101	828	288	1101
05-Dec-12	100	200	100	100	100	100	100
15-Dec-00*	388	400	531	1075	799	445	1075
15-Dec-12*	238	400	349	100	100	100	100
16-Dec-00*	100	100	367	415	415	156	415
24-Dec-12*	100	100	100	100	100	100	100
25-Dec-00	5000	300	361	606	606	156	606
25-Dec-12*	100	100	100	100	100	100	100

Appendix G. Mixed Layer Heights For Grand Junction, CO

Table 25 contains the subjective and algorithm mixed layer heights using observed soundings from calendar year 1996. The following abbreviations were used in the table: OBS is the subjective height, RI is RICH, PO is POTEMP, PI d/n is PIMIX day/night, and PI is PIMIX. Heights are reported in meters AGL. Dates with an asterisk represent the easy cases used to calculate the algorithm RMSE.

Table 25 Mixed layer heights for Grand Junction using observed soundings.

Date/Time (UTC)	OBS	RICH	POTEMP	PIMIX d/n	PIMIX
10-Jan-00*	250	-500	381	381	381
10-Jan-12*	100	100	100	100	100
11-Jan-00	75	1100	2773	2773	2773
19-Jan-12*	100	-500	100	100	100
20-Jan-00*	575	-500	700	1426	1426
20-Jan-12	1825	100	2008	100	2007
30-Jan-00*	225	-500	381	380	380
30-Jan-12	2775	-500	2961	100	2960
31-Jan-00	100	-500	100	100	100
08-Feb-12	100	100	502	100	501
09-Feb-00*	500	600	758	713	713
09-Feb-12*	100	-500	100	100	100
19-Feb-00	5000	400	2838	6731	6731
19-Feb-12*	100	400	100	100	100
20-Feb-00	475	600	1804	3329	3329
28-Feb-12	2075	100	727	100	2228
29-Feb-00	1825	2300	4131	4130	4130
29-Feb-12	3325	100	1317	100	1391
10-Mar-00*	1225	1000	1370	1327	1327
10-Mar-12*	100	100	730	100	100
11-Mar-00	675	400	957	2557	2557
19-Mar-12	775	100	890	100	861
20-Mar-00*	1275	700	1508	2081	2081
20-Mar-12*	1525	100	617	100	617
30-Mar-00	1225	2200	1479	6542	6542

Table 25 cont.

Date-Time (UTC)	OBS	RI	PO	PI d/n	PI
30-Mar-12*	100	1100	120	120	120
31-Mar-00*	2475	400	2688	2753	2753
08-Apr-12*	100	100	100	100	100
09-Apr-00	5000	-500	3423	8702	8702
09-Apr-12*	100	100	100	100	100
19-Apr-00	5000	-500	816	12519	12519
19-Apr-12*	2550	1600	2740	100	2740
20-Apr-00*	3200	-500	3402	3445	3445
28-Apr-12	100	100	3436	100	4740
29-Apr-00	5000	700	5870	5934	5934
29-Apr-12	100	100	2640	100	2640
09-May-00	5000	700	5576	5680	5680
09-May-12*	100	-500	4156	100	7164
10-May-00	5000	1300	4422	8891	8891
18-May-12	3225	100	3344	3327	3327
19-May-00	5000	1300	4803	4802	4802
19-May-12	2900	100	874	829	829
29-May-00	m	-500	31295	100	100
29-May-12*	100	-500	1261	1226	1226
30-May-00	5000	-500	4261	4231	4231
07-Jun-12	1825	-500	100	1913	1913
08-Jun-00	5000	1300	5291	11255	11255
08-Jun-12*	100	100	100	100	100
18-Jun-00	5000	3600	5348	5381	5381
18-Jun-12*	100	100	8890	100	100
19-Jun-00	3325	-500	8412	8594	8594

Table 25 cont.

Date-Time (UTC)	OBS	RI	PO	PI d/n	PI
27-Jun-12	3475	400	3927	3972	3972
28-Jun-00*	225	-500	417	383	383
28-Jun-12	100	400	4526	4526	4526
08-Jul-00	5000	400	4708	5918	5918
08-Jul-12	100	100	4675	5202	5202
09-Jul-00	5000	400	4126	4126	4126
17-Jul-12	100	100	100	100	4710
18-Jul-00	125	200	194	232	232
18-Jul-12*	100	400	100	100	100
28-Jul-00	5000	1300	4888	4888	4888
28-Jul-12	m	-500	-500	-500	-500
29-Jul-00*	950	1000	1097	1097	1097
06-Aug-12*	100	100	3382	100	5003
07-Aug-00	5000	3200	3923	8111	8111
07-Aug-12	5000	100	4962	100	5057
17-Aug-00	5000	1000	3937	3966	3966
17-Aug-12	925	400	982	100	966
18-Aug-00	5000	2300	4697	6377	6377
26-Aug-12	5000	100	8979	100	8930
27-Aug-00	1125	700	3958	5857	5857
27-Aug-12*	100	100	2920	100	2919
06-Sep-00	2225	400	97	3013	3013
06-Sep-12	100	-500	2508	100	2507
07-Sep-00	5000	700	789	4765	4765
15-Sep-12	100	100	1207	100	1207
16-Sep-00	2675	700	2177	2787	2787

Table 25 cont.

Date-Time	OBS	RI	PO	PI d/n	PI
16-Sep-12*	100	200	3237	100	3236
26-Sep-00	5000	800	4047	4046	4046
26-Sep-12*	100	100	2490	100	2441
27-Sep-00	5000	-500	4746	4817	4817
05-Oct-12	100	100	100	100	2877
06-Oct-00	525	600	763	2698	2698
06-Oct-12	100	100	100	100	1077
16-Oct-00	2800	400	2996	2995	2995
16-Oct-12*	100	-500	3506	100	100
17-Oct-00	1325	700	1541	1540	1540
25-Oct-12	5000	-500	1730	1955	1955
26-Oct-00	350	100	539	539	539
26-Oct-12	5000	1100	1727	100	2934
05-Nov-00*	1925	400	2078	2103	2103
05-Nov-12	100	-500	2659	100	4109
06-Nov-00	5000	100	976	4559	4559
14-Nov-12*	100	100	100	100	100
15-Nov-00	100	100	100	4367	4367
15-Nov-12*	300	500	438	438	438
25-Nov-00	725	200	1250	1991	1991
25-Nov-12*	100	100	100	100	100
26-Nov-00	1725	-500	2004	2093	2093
04-Dec-12	100	-500	1543	100	3180
05-Dec-00	1575	-500	1517	1517	1517
05-Dec-12	100	200	1313	100	1312

Table 25 cont.

Date-Time (UTC)	OBS	RI	PO	PI d/n	PI
15-Dec-00*	2800	2500	3522	3522	3522
15-Dec-12	5000	-500	2600	2661	2661
16-Dec-00	750	1500	1031	1101	1101
24-Dec-12	100	100	2030	100	2030
25-Dec-00*	100	100	100	100	100
25-Dec-12*	100	100	100	100	100

Table 26 contains the subjective and algorithm mixed layer heights using RAMS soundings from calendar year 1996. The following abbrěviations were used in the table: OBS is the subjective height, RI is RICH, PO is POTEMP, PD is PIMIX day/night, P1 is PIMIX-NM1, P2 is PIMIX-NM2, and PI is PIMIX. Heights are reported in meters AGL. Dates with an asterisk represent the easy cases used to calculate the algorithm RMSE.

Table 26 Mixed layer heights for Grand Junction using RAMS soundings.

Date-Time (UTC)	OBS	RI	PO	PD	P1	P2	PI
10-Jan-00	125	100	323	405	405	146	405
10-Jan-12*	100	200	437	100	100	100	100
11-Jan-00*	225	100	423	793	793	268	793
19-Jan-12	225	-500	336	413	413	146	413
20-Jan-00*	125	300	411	792	792	146	792
20-Jan-12	100	1500	380	100	100	100	100
30-Jan-00	400	100	509	767	767	414	767
30-Jan-12*	125	200	407	2020	2020	146	2020
31-Jan-00	275	200	525	793	793	268	793
08-Feb-12*	100	100	100	100	100	100	100
09-Feb-00*	375	300	638	758	758	414	758
09-Feb-12*	100	200	100	100	100	100	100
19-Feb-00	5000	1500	2973	6241	6241	6241	6241
19-Feb-12*	100	100	100	100	100	100	100

Table 26 cont.

Date-Time (UTC)	OBS	RI	PO	PD	P1	P2	PI
20-Feb-00*	400	300	679	3668	3668	414	3668
28-Feb-12	375	100	617	779	779	268	779
01-Mar-00	575	700	2002	2592	2592	2592	2592
01-Mar-12	100	200	231	2949	100	100	2949
10-Mar-00	775	500	1061	1266	1266	1266	1266
10-Mar-12*	100	200	100	100	100	100	100
11-Mar-00*	425	500	610	726	726	414	726
19-Mar-12	125	200	341	100	531	146	531
20-Mar-00	575	500	864	1636	1639	1639	1636
20-Mar-12*	100	200	100	100	100	100	100
30-Mar-00*	1025	900	1346	6313	6313	6313	6313
30-Mar-12	5000	300	217	2446	100	100	2446
31-Mar-00	575	400	2435	4642	4535	4535	4642
08-Apr-12	125	100	328	526	526	146	526
09-Apr-00*	575	600	3601	8640	8425	8425	8640
09-Apr-12*	100	200	100	100	100	100	726
19-Apr-00	5000	1600	2433	5432	5427	5427	5432
19-Apr-12	825	500	1082	3005	100	100	3005
20-Apr-00*	400	500	2913	3066	3066	3066	3066
28-Apr-12	5000	1200	703	1041	1041	414	1041
29-Apr-00	2125	-500	3605	3801	3801	3801	3801
29-Apr-12*	100	300	554	100	100	100	100
09-May-00	5000	-500	8958	8600	8366	8366	8600
09-May-12	5000	200	701	6424	6405	6405	6424
10-May-00	5000	2200	4561	7435	7435	7435	7435
18-May-12	5000	2800	356	551	551	146	551

Table 26 cont.

Date-Time (UTC)	OBS	RI	PO	PD	P1	P2	PI
19-May-00	3325	-500	2936	10063	10063	10063	10063
19-May-12	5000	-500	2941	5287	5287	5287	5287
29-May-00*	625	300	793	793	793	793	793
29-May-12	775	100	659	1025	1025	1025	1025
30-May-00	5000	2300	6148	6397	6321	6321	6397
07-Jun-12*	100	100	264	396	396	146	396
08-Jun-00	5000	400	2028	9329	9285	9285	9329
08-Jun-12*	625	200	100	749	749	749	749
18-Jun-00	5000	-500	5209	6504	7269	7269	6504
18-Jun-12	100	300	240	7314	7314	7314	7314
19-Jun-00	5000	500	8430	8614	8223	8223	8614
27-Jun-12	125	100	340	560	560	146	560
28-Jun-00	400	2200	3576	6391	6194	6194	6391
28-Jun-12	225	500	487	579	579	579	579
17-Jul-12	325	100	373	578	578	268	578
18-Jul-00	5000	600	3589	9189	9158	9158	9189
18-Jul-12*	375	400	657	100	749	749	749
28-Jul-00	5000	100	5222	9197	9179	9179	9197
28-Jul-12	100	900	524	100	100	100	9199
29-Jul-00*	525	500	649	9187	9157	9157	9187
06-Aug-12	100	100	100	559	559	146	559
07-Aug-00*	1525	1400	7991	8519	8127	8127	8519
07-Aug-12	100	100	547	100	100	100	7273
17-Aug-00	3325	1800	3576	9164	9136	9136	9164
17-Aug-12	5000	100	548	100	100	100	9098
18-Aug-00	5000	100	5192	9133	8251	8251	9133

Table 26 cont.

Date-Time (UTC)	OBS	RI	PO	PD	P1	P2	PI
26-Aug-12	425	100	503	100	741	414	741
27-Aug-00	5000	100	3554	8124	8104	8104	8124
27-Aug-12	525	300	524	781	781	781	781
06-Sep-00*	100	100	100	100	100	100	100
06-Sep-12	5000	100	239	5288	5288	5288	5288
07-Sep-00	5000	700	2937	5278	5278	5278	5278
15-Sep-12*	100	100	100	100	100	100	100
16-Sep-00	525	500	795	8606	8298	8298	8606
16-Sep-12*	100	300	100	100	100	100	100
26-Sep-00	5000	1200	3542	6318	6318	6318	6318
26-Sep-12	5000	100	2435	100	100	100	4481
27-Sep-00	5000	1500	3543	3697	3697	3697	3697
05-Oct-12*	100	200	100	100	100	100	100
06-Oct-00	5000	300	647	8643	8277	8277	8643
06-Oct-12*	100	200	100	100	100	100	100
16-Oct-00	5000	3400	2951	8658	8412	8412	8658
16-Oct-12	5000	200	8948	100	100	100	4600
17-Oct-00	5000	500	500	4524	4403	4403	4524
25-Oct-12	5000	900	517	768	768	414	768
26-Oct-00*	275	200	512	6302	6302	268	6302
26-Oct-12	125	400	523	4636	1698	268	4636
05-Nov-00	1725	200	413	1900	1900	590	1900
05-Nov-12*	100	300	535	100	100	100	100
06-Nov-00	5000	900	413	3682	3682	3682	3682
14-Nov-12*	100	100	100	100	100	100	100
15-Nov-00*	375	300	480	568	568	268	568

Table 26 cont.

Date-Time (UTC)	OBS	RI	PO	PD	P1	P2	PI
15-Nov-12	575	200	820	1340	1340	590	1340
25-Nov-00	5000	200	855	1026	1026	414	1026
25-Nov-12	525	100	323	100	100	100	100
26-Nov-00	625	100	553	100	6533	268	6533
04-Dec-12*	100	100	100	100	100	100	100
05-Dec-00	400	200	639	1041	1041	414	1041
05-Dec-12	100	300	128	127	100	100	127
15-Dec-00	5000	700	3605	3678	3678	3678	3678
15-Dec-12	5000	400	539	100	100	100	2102
16-Dec-00*	225	100	856	1027	1027	414	1027
24-Dec-12*	100	300	100	100	100	100	100
25-Dec-00*	375	200	510	780	780	268	780
25-Dec-12*	100	200	100	100	100	100	100

Appendix H. Mixed Layer Heights for North Platte, NE

Table 27 contains the subjective and algorithm mixed layer heights using observed soundings from calendar year 1996. The following abbreviations were used in the table: OBS is the subjective height, RI is RICH, PO is POTEMP, PI d/n is PIMIX day/night, and PI is PIMIX. Heights are reported in meters AGL. Dates with an asterisk represent the easy cases used to calculate the algorithm RMSE.

Table 27 Mixed layer heights for North Platte using observed soundings.

Date-Time (UTC)	OBS	RI	PO	PI d/n	PI
10-Jan-00*	463	500	511	511	511
10-Jan-12	138	500	176	100	175
11-Jan-00	313	500	545	2103	2103
19-Jan-12	788	600	873	872	872
20-Jan-00*	313	600	576	575	575
20-Jan-12	100	200	-500	100	1386
30-Jan-00	188	300	290	892	892
30-Jan-12	3438	100	913	100	2371
31-Jan-00	388	300	468	587	587
08-Feb-12*	100	100	3505	100	100
09-Feb-00*	138	200	178	195	195
09-Feb-12*	313	400	370	369	369
19-Feb-00*	88	300	134	133	133
19-Feb-12	1788	300	1919	1919	1919
20-Feb-00	5000	1600	607	1618	1618
28-Feb-12*	100	100	1906	100	1927
29-Feb-00	2488	500	2107	2487	2487
29-Feb-12*	100	-500	2068	100	2068
10-Mar-00*	388	400	413	412	412
10-Mar-12*	100	100	553	100	1700
11-Mar-00	313	400	599	551	551
19-Mar-12	238	300	290	289	289
20-Mar-00	163	200	196	196	196
20-Mar-12*	100	100	46	46	46
30-Mar-00*	338	400	363	377	377

Table 27 cont.

Date-Time (UTC)	OBS	RI	PO	PI d/n	PI
30-Mar-12	100	400	365	100	364
31-Mar-00*	513	200	614	677	677
09-Apr-00*	563	600	606	605	605
09-Apr-12*	938	600	996	100	1029
19-Apr-00*	463	900	562	561	561
19-Apr-12	100	300	1533	100	1532
20-Apr-00*	388	700	256	481	481
28-Apr-12*	100	100	100	100	100
29-Apr-00*	138	200	155	163	163
29-Apr-12*	100	200	100	100	100
09-May-00	238	300	259	312	312
09-May-12	238	300	250	250	250
10-May-00*	288	300	304	303	303
18-May-12*	100	1000	999	100	999
19-May-00	863	200	211	249	249
19-May-12	5000	300	280	1085	1085
29-May-00*	588	-500	-500	-500	-500
29-May-12*	938	1000	951	951	951
30-May-00*	738	500	761	763	763
07-Jun-12*	100	100	100	100	100
08-Jun-00*	288	100	339	347	347
08-Jun-12	100	300	179	180	180
18-Jun-00*	100	-500	-500	100	100
18-Jun-12	1488	200	100	100	100
19-Jun-00	188	300	201	200	200
27-Jun-12	100	100	617	100	924

Table 27 cont.

Date-Time (UTC)	OBS	RI	PO	PI d/n	PI
28-Jun-00*	388	400	526	526	526
28-Jun-12	263	300	249	248	248
08-Jul-00*	738	400	345	345	345
08-Jul-12*	288	400	335	334	334
09-Jul-00*	313	400	338	340	340
17-Jul-12	488	100	506	100	528
18-Jul-00*	438	500	452	451	451
18-Jul-12*	100	400	100	100	100
28-Jul-00*	263	-500	278	277	277
28-Jul-12	238	100	247	100	247
29-Jul-00*	188	200	189	188	188
06-Aug-12	838	200	603	602	602
07-Aug-00*	463	500	528	528	528
07-Aug-12*	488	100	275	538	538
17-Aug-12*	288	100	295	294	294
18-Aug-00*	313	400	337	339	339
26-Aug-12	738	300	523	522	522
27-Aug-00*	163	500	212	211	211
27-Aug-12*	138	200	158	157	157
06-Sep-00*	238	300	256	256	256
06-Sep-12*	100	200	100	100	100
07-Sep-00	100	100	642	619	619
15-Sep-12	1188	400	-500	847	847
16-Sep-00*	213	300	-500	304	304

Table 27 cont.

Date-Time (UTC)	OBS	RI	PO	PI d/n	PI
16-Sep-12*	100	300	679	100	729
26-Sep-00*	563	300	582	589	589
26-Sep-12*	538	300	575	574	574
27-Sep-00*	388	400	420	419	419
05-Oct-12*	100	100	100	100	100
06-Oct-00*	100	100	100	100	100
06-Oct-12*	100	100	100	100	100
16-Oct-00*	38	200	74	73	73
16-Oct-12	138	200	100	100	100
17-Oct-00	100	200	1242	100	100
25-Oct-12	100	300	767	100	1116
26-Oct-00*	788	600	935	935	935
26-Oct-12	100	-500	1479	100	1711
05-Nov-00*	538	800	681	786	786
05-Nov-12	938	300	957	100	957
06-Nov-00*	263	300	343	330	330
14-Nov-12*	213	300	257	256	256
15-Nov-00*	163	600	237	236	236
15-Nov-12	513	300	561	560	560
25-Nov-00*	88	200	125	124	124
25-Nov-12*	100	300	210	100	210
26-Nov-00*	138	300	181	181	181
04-Dec-12*	288	300	353	100	384
05-Dec-00*	88	200	153	153	153
05-Dec-12*	100	100	1411	100	1393
15-Dec-00*	188	300	284	284	284

Table 27 cont.

Date-Time (UTC)	OBS	RI	PO	PI d/n	PI
15-Dec-12*	100	200	2903	100	2857
16-Dec-00*	100	100	100	100	100
24-Dec-12*	100	100	100	100	100
25-Dec-00	88	300	171	671	671
25-Dec-12*	100	100	270	100	269

Table 28 contains the subjective and algorithm mixed layer heights using RAMS soundings from calendar year 1996. The following abbreviations were used in the table: OBS is the subjective height, RI is RICH, PO is POTEMP, PD is PIMIX day/night, P1 is PIMIX-NM1, P2 is PIMIX-NM2, and PI is PIMIX. Heights are reported in meters AGL. Dates with an asterisk represent the easy cases used to calculate the algorithm RMSE.

Table 28 Mixed layer heights for North Platte using RAMS soundings.

Date-Time (UTC)	OBS	RI	PO	PD	P1	P2	PI
10-Jan-00	5000	200	100	650	689	689	650
10-Jan-12	100	600	579	100	100	100	579
11-Jan-00	651	600	578	100	100	100	578
19-Jan-12*	100	100	555	222	222	222	222
20-Jan-00*	326	400	488	100	100	100	327
20-Jan-12*	100	100	508	100	100	100	100
30-Jan-00	100	100	562	100	100	100	562
30-Jan-12*	100	400	561	348	348	348	348
31-Jan-00*	476	600	571	571	496	496	571
08-Feb-12*	100	700	597	100	100	100	597
09-Feb-00	451	600	586	586	907	907	586
09-Feb-12*	100	400	580	100	100	100	100
19-Feb-00	2751	600	490	489	8984	8984	489
19-Feb-12*	100	300	483	100	100	100	482
20-Feb-00	651	600	462	461	9942	9942	461
28-Feb-12	451	100	100	100	492	492	100
01-Mar-00*	651	800	100	635	686	686	635

Table 28 cont.

Date-Time (UTC)	OBS	RI	PO	PD	P1	P2	PI
01-Mar-12*	100	100	100	100	100	100	100
10-Mar-00*	1801	800	100	669	1849	1849	669
10-Mar-12*	100	300	100	100	100	100	100
11-Mar-00	476	800	100	512	512	512	512
19-Mar-12	551	700	707	2082	7082	7082	2082
20-Mar-00*	1126	800	100	623	8991	8991	623
20-Mar-12*	100	300	100	100	100	100	100
30-Mar-00	100	100	405	736	604	151	736
30-Mar-12	100	300	100	100	100	100	100
31-Mar-00	596	900	838	998	998	608	998
08-Apr-12*	100	100	100	100	100	100	100
09-Apr-00	2251	2900	2494	9487	9454	9454	9487
09-Apr-12*	100	100	100	100	100	100	100
19-Apr-00	5000	100	7280	7447	7447	7447	7447
19-Apr-12	100	400	869	4595	4587	608	4595
20-Apr-00	1151	1200	1696	3828	3828	3828	3828
28-Apr-12*	476	100	593	593	9941	9941	593
29-Apr-00	5000	800	100	626	8038	8038	626
29-Apr-12*	100	300	100	651	8988	8988	651
09-May-00	451	100	422	801	801	801	801
09-May-12	5000	300	100	755	755	427	755
10-May-00	651	1500	756	771	755	755	771
18-May-12*	100	100	100	100	100	100	100
19-May-00	5000	1000	758	9468	8489	8489	9468
19-May-12*	100	300	100	100	100	100	100

Table 28 cont.

Date-Time (UTC)	OBS	RI	PO	PD	P1	P2	PI
29-May-00*	651	200	876	1006	1006	608	1006
29-May-12*	100	100	100	100	100	100	100
30-May-00*	1101	1500	1274	1273	1273	1273	1273
07-Jun-12	651	1200	868	1027	1027	608	1027
08-Jun-00*	1401	1000	1555	1554	1554	1554	1554
08-Jun-12*	100	100	100	100	100	100	100
18-Jun-00*	851	700	1065	8401	8392	8392	8401
18-Jun-12	100	300	100	559	559	559	559
19-Jun-00*	1451	800	1668	8450	8446	8446	8450
27-Jun-12	301	900	375	585	585	276	585
28-Jun-00*	1101	1100	1343	10727	11352	11352	10727
28-Jun-12*	326	500	500	607	607	607	607
17-Jul-12	251	900	100	547	548	151	547
18-Jul-00*	1426	900	3645	10704	10455	10455	10704
18-Jul-12	201	300	321	425	425	151	425
06-Aug-12*	100	100	100	364	364	151	364
07-Aug-00*	1426	1900	1689	8388	8394	8394	8388
07-Aug-12*	176	700	345	966	772	151	966
17-Aug-00	651	500	1344	9427	9427	9427	9427
17-Aug-12	451	200	100	575	575	276	575
18-Aug-00*	1101	700	1274	1274	1274	1274	1274
26-Aug-12*	100	100	100	100	100	100	100
27-Aug-00*	1426	1100	1318	7421	7421	7421	7421
27-Aug-12	100	300	669	100	100	100	824
06-Sep-00	5000	1000	1697	9383	8426	8426	9383
06-Sep-12*	100	300	100	100	100	100	100

Table 28 cont.

Date-Time (UTC)	OBS	RI	PO	PD	P1	P2	PI
07-Sep-00*	851	900	1065	9513	9513	9513	9513
15-Sep-12	5000	100	100	566	566	151	566
16-Sep-00*	301	300	454	566	566	276	566
16-Sep-12*	151	300	256	256	256	256	256
26-Sep-00	601	200	395	726	726	427	726
26-Sep-12	5000	300	543	100	100	100	789
27-Sep-00*	1126	1200	1364	5598	5598	5598	5598
05-Oct-12*	451	500	459	547	547	276	547
06-Oct-00*	851	900	1047	9543	9543	9543	9543
06-Oct-12*	100	200	100	100	100	100	100
16-Oct-00	5000	100	553	977	977	608	977
16-Oct-12*	100	200	100	100	100	100	100
17-Oct-00*	651	500	789	789	789	789	789
25-Oct-12*	100	100	100	100	100	100	100
26-Oct-00*	651	700	827	990	990	608	990
26-Oct-12	100	400	891	100	100	100	1064
05-Nov-00	651	1100	437	1064	1064	608	1064
05-Nov-12*	100	100	100	100	100	100	100
06-Nov-00	451	100	656	789	789	427	789
14-Nov-12	451	700	476	532	532	276	532
15-Nov-00*	301	700	456	538	537	276	538
15-Nov-12*	100	900	100	100	100	100	100
25-Nov-00	351	100	415	415	415	415	415
25-Nov-12*	100	100	100	100	100	100	100
26-Nov-00	426	100	416	415	415	415	415
04-Dec-12*	100	100	100	100	100	100	100

Table 28 cont.

Date-Time (UTC)	OBS	RI	PO	PD	P1	P2	PI
05-Dec-00	100	500	651	100	100	100	3848
05-Dec-12*	100	300	100	100	100	100	100
15-Dec-00	651	900	530	813	813	427	813
15-Dec-12*	100	300	100	100	100	100	100
16-Dec-00*	100	700	558	100	100	100	100
24-Dec-12*	100	100	100	100	100	100	100
25-Dec-00*	176	-500	285	368	368	151	368
25-Dec-12*	100	100	100	100	100	100	100

Appendix I. GEMPAK SNPROF Program Example

The GEMPAK program used in this research was SNPROF, which generates graphics from upper air observational data. To aid in estimating the PBL height, two SNPROF parameters were plotted: virtual potential temperature and skewt-T. A detailed explanation of SNPROF can be found in Chapter 4 of the N-AWIPS User's Guide. The following is an example of the graphics design for a plot of the virtual potential temperature parameter for Vandenburg AFB, CA on 9 Apr 96 at 00 UTC, as depicted in Figure 8.

SNFILE Sounding data file /home/snds/all_obs.snd

DATTIM Date/time 960409/00

AREA Data area vbg

SNPARM Sounding parameter list THTV

VCOORD Vertical coordinate type HGHT

WIND Wind symbol/siz/wdth/typ/hdsz BM1

WINPOS Wind position 1

DEVICE Device XW

YAXIS Ystrt/ystop/yinc/lbl;gln;tck 850/5050/100

XAXIS Xstrt/xstop/xinc/lbl;gln;tck

THTALN THTA color/dash/width/mn/mx/inc 8

THTELN THTE color/dash/width/mn/mx/inc 23

MIXRLN MIXR color/dash/width/mn/mx/inc 23/3

To calculate and plot virtual potential temperature, GEMPAK uses the following equations (18: NCEP 1996):

$$MIXR = .622(\frac{E}{P-E})1000 \tag{12}$$

where MIXR is the mixing ratio, E is vapor pressure, and P is atmospheric pressure,

$$TVRK = TMPK\frac{\left[1 + \frac{(.001MIXR)}{.622}\right]}{[1 + (.001MIXR)]} \tag{13}$$

where TVRK is virtual temperature (K) and TMPK is temperature (K) and,

$$THTV = TVRK(\frac{1000}{P})^{K} \tag{14}$$

where THTV is virtual potential temperature and K is Poisson's constant defined by $(\frac{R_d}{C_p}) \approx \frac{2}{7} \approx .286$

Bibliography

1. Alapaty K., J. E. Pleim, S. Raman D. S. Niyogi and D. W. Byun. "Simulation of Atmospheric Boundary Layer Processes Using Local- and Nonlocal-Closure Schemes," *Journal of Applied Meteorology*, *36*:214–233 (1997).

2. Andre, J. C., G. De Moor P. Lacarrere G. Therry and R. Du Vachat. "Modeling the 24-Hour Evolution of the Mean and Turbulent Structures of the Planetary Boundary Layer," *Journal of the Atmospheric Sciences*, *35*:1861–1883 (1978).

3. Brooks, H. E. and C. A. Doswell III. "A Comparison of Measures-Oriented and Distributions-Oriented Approaches to Forecast Verification," *Weather and Forecasting*, *11*:288–303 (1996).

4. Capuano, M. E., M. A. Kienzle and W. L. Steorts. *Short Range Atmospheric Model (SLAM) Technical Description*. Technical Report, 445 Pineda Court, Melbourne, FL 32940: ENSCO, INC., 1997.

5. Capuano, M. E. and M. K. Atchison. *Worldwide Climatalogical Maximum Mixed Layer Heights*. Technical Report, 445 Pineda Court, Melbourne, FL 32940: ENSCO, INC., 1985.

6. Conover, W. J. *Practical Non-Parametric Statistics* (Second Edition). John Wiley and Sons, 1980.

7. Dayan, U. and J. Rodnizki. "The Temporal Behavior of the Atomospheric Boundary Layer in Israel," *Journal of Applied Meteorology*, *38*:830–836 (1998).

8. Deardorff, J. W. "Three-Dimensional Numerical Study of the Height and Mean Structure of a Heated Planetary Boundary Layer," *Boundary Layer Meteorology*, *7*:81–106 (1974).

9. Devore, J. L. *Probability and Statistics for Engineering and the Sciences* (Fourth Edition). Duxbury Press, 1995.

10. Dunn, O. J. "Multiple Comparisons Among Means," *American Statistical Association Journal*, *56*:52–64 (1961).

11. Fleagle, R. G. and J. A . Businger. *An Introduction to Atomospheric Physics* (second Edition). Academic Press, Inc., 1980.

12. Garratt, J. R. *The Atomospheric Boundary Layer*. Cambridge University Press, 1992.

13. Holton, J. R. *Introduction to Dynamic Meteorology* (Third Edition). Academic Press, 1992.

14. Hooper, William P. and Edwin W. Eloranta. "Lidar Measurements of Wind in the Planetary Boundary Layer: The Method, Accuracy, and Results from Joint Measurements with Radiosonde and Kytoon," *Journal of Climate and Applied Meteorology*, *25*:990–1001 (1986).

15. Kaimal, J. C., J. C. Wyngaard D. A. Haugen O. R. Cote Y. Izumi S. J. Caughey and C. J. Readings. "Turbulence Structure in the Convective Boundary Layer," *Journal of the Atmospheric Sciences*, *33*:2152–2169 (1976).

16. Kienzle, M. A. and S. E. Masters. *Deveolpment and Application of the Potential Instability Mixing Depth Estimation Technique (PIMIX)*. Technical Report, 445 Pineda Court, Melbourne, FL 32940: ENSCO, INC., 1990.

17. Marascuilo, L. A. and M. McSweeny. *Nonparametric and Distribution-Free Methods for the Social Sciences*. Wadsworth Publishing Co., 1977.

18. National Centers for Environmental Prediction (NCEP). *N-AWIPS User's Guide, Version 5.4*, October 1996.

19. Russ, R. L. *Estimating the Height of the Planetary Boundary Layer for Diffusion-Transport Atmospheric Models: A Four Algorithm Comparison*. MS thesis, Air Force Institute of Technology, 1999.

20. Slonaker, R. L., B. E. Schwartz and W. J. Emery. "Occurrence of Nonsurface Superadiabatic Lapse Rates Within RAOB Data," *Weather and Forecasting*, *11*:350–359 (1996).

21. Stull, Roland B. *An Introduction to Boundary Layer Meteorology*. Kluwer Academic Publishers, 1988.

22. Walko, R. L., C. J. Tremback and R. F. A. Hertenstein. *RAMS: The Regional Atmospheric Modeling System, Version 3a, Users Guide*. ASTeR, Inc., P.O. Box 466, Ft. Collins, CO 80522, 1993.

23. Wilks, D. S. *Statistical Methods in the Atmospheric Sciences*. Academic Press, 1995.

24. Wyngaard, J. C. *On Boundary Layer Measurement Physics, Probing the Atmospheric Boundary Layer.*. The American Meteorological Society, 1986.

Vita

Captain Lisa C. Shoemaker was born 8 January 1969 in Jefferson City, MO, and she graduated from Cushing High School, OK in 1987. In 1991, she was awarded a Bachelor of Science in Mathematics from Angelo State University in San Angelo, TX, and was commissioned a second lieutenant through Air Force ROTC. Her first assignment was as a student in the Air Force Institute of Technology Basic Meteorology Program at Texas A&M University, where she received a Bachelor of Science in Meteorology. Following graduation from Texas A&M in 1993, Captain Shoemaker got her first operational assignment as Wing Weather officer at Dyess AFB TX, where she supported C-130, KC-135, and B-1B aircraft. Her assignment to Dyess afforded her opportunities to deploy with B1-B aircraft to England for a multinational exercise and to serve as officer in charge of a weather team deployed to Mombasa, Kenya, during Operation SUPPORT HOPE - Rwanda humanitarian relief effort.

In 1995, Captain Shoemaker was assigned to Scott AFB, IL as a wing weather officer and was quickly selected to serve as squadron mobility officer and squadron executive officer. Once again, deployment opportunities arose, and Captain Shoemaker was twice temporarily assigned to Moron AB, Spain, to support airlift and air refueling operations. Following completion of Squadron Officer's School in August 1997, she was selected for assignment as the Assistant Chief of Weather Readiness, Headquarters Air Mobility Command Division of Weather, where her duties included sourcing weather personnel and equipment for command operational readiness inspections and worldwide contingencies. In March 1998, she was selected to attend the Air Force Institute of Technology to pursue a master of Science degree in Meteorology. Following graduation, Captain Shoemaker will be assigned to the Air Force Technical Applications Center, Patrick AFB, FL.

Permanent address: 107 Hwy 5, Lot O
Gravois Mills, MO 65037